Preparation and Properties of Strips produced from High Energy Milled Copper & Tungsten Powders via a Powder Metallurgy Route

A thesis submitted

In partial fulfillment of the requirements

For the degree of

MASTER OF TECHNOLOGY

By

RAJESH SHARMA

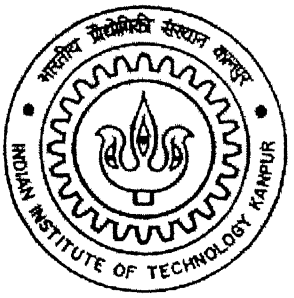

DEPARTMENT OF MATERIALS & METALLURGICAL ENGINEERING

INDIAN INSTITUTE OF TECHNOLOGY, KANPUR

May 2002

CERTIFICATE

This is to certify that the thesis entitled **" Preparation and Properties of Strips Produced from High Energy Milled Copper and Tungsten Powders via a Powder Metallurgy Route "**submitted by Mr. Rajesh Sharma, has been carried out in my supervision and has not been submitted elsewhere for a degree.

R. K. Dube
Professor,
Department of Materials and Metallurgical Engg.,
Indian Institute of Technology,
Kanpur 208016.

ABSTRACT

A new Powder Metallurgy route has been proposed for making Copper-Tungsten composite strips. The route consists of milling a mixture of copper and tungsten powders in the required ratio in a high energy ball mill. The resulting powder is mixed with a binder to form a homogeneous and free flowing slurry. Strips are cast from this slurry, and are subsequently dried to form coherent Copper-Tungsten composite strips. The strips are sintered at a suitable temperature, and are subsequently hot rolled followed by an annealing treatment. Percent thickness reduction by hot rolling has been optimized for providing strip having good mechanical properties. It has been shown that it is possible to produce 80Cu-20W strip having an ultimate tensile strength of 281 MPa, 0.2% proof strength of 104 MPa, elongation of 21% together with an electrical conductivity of 76% IACS. The mechanisms of densification and deformation occurring during hot rolling have been also studied. The effect of tungsten in the range 5 wt%-20 wt% on the mechanical properties, porosity, and electrical conductivity of the hot rolled annealed strip have also been investigated.

ACKNOWLEDGEMENT

I would like to express my deep sense of gratitude to my thesis supervisor Dr. R. K. Dube for their expert guidance and support that encouraged me to overcome problems experienced during my thesis work. Their help in final thesis preparation is unforgettable.

I am thankful to Mr. S. C. Soni for providing guidance during experimental work.

I convey my thanks to all my friends who gave moral support throughout my graduate studies.

I am also thankful to all the staff of Materials and Metallurgical Engineering Department and Advanced Center for Materials Science, for their unconditional help.

RAJESH SHARMA

Contents

Page No.

List of Figures

Page No.

List of Tables

CHAPTER 1

INTRODUCTION

Electrical contact materials are metal devices that make and break electrical circuits. They are mainly used as air and oil circuit breakers, aircraft switches, sliding contacts etc. They are also used for thermal management applications and in semiconductor industries. The main problems in the application of electrical contact materials are arcing, oxidation and welding. Arcing is the major factor causing failure of contact points. The arc causes contact erosion by blowing away the molten metal droplets and vaporizing the material. Oxidation of contact surfaces will be higher if the metallic oxide films are non-conductive. This oxide may easily increase contact resistance. Temperature rise due to generation of large amount of heat causes welding of the contacts. To overcome the above problems, copper-tungsten composite contact material is used. The other contact materials are Cu-Mo, Cu-Al_2O_3, Ag-Mo, Ag-W, Ag-CdO, etc[1] [2] [3].

Depending upon the applications and compositions of electrical contact materials, they are produced in various shapes. Except for tungsten and molybdenum, electrical contact materials are ductile enough so that they can be produced in all contact forms. Tungsten and molybdenum and some of the powder metallurgy materials have lower ductility and are available in fewer forms. The commercially available forms of common electrical contact materials are rivet, wire, strip, tape, disks, clad, rings and bushes[4].

The selection of electrical contact materials depends upon their properties[5].The desired properties include high electrical conductivity, high thermal conductivity to dissipate both the resistive and arc heat developed, high resistance to chemical reactions. The melting point of electrical contact materials should be high enough to limit arc erosion, metal transfer and welding but low enough to increase resistance to reignition in switching. Hardness should be high to provide good wear resistance. High electrical and thermal conductivity of Cu account for the wide use of Cu in electrical contacts. However it does not provide high resistance to arcing, welding or sticking. If pure copper is used, then weld

strength will be high even at low current so making and breaking of contacts is difficult. With addition of tungsten, weld strength is low even at high current, which facilitates the making and breaking of circuit easily. Due to these limitations, Cu-W is used as contact materials where high hardness at both room and elevated temperatures are desirable. Cu and W have no solid solubility as shown in the phase diagram (Fig. 1.1) and could be considered as a metal-metal composite. Due to lack of solubility of tungsten in copper, and high melting point of tungsten, liquid technology method is not adopted for its manufacture. Powder metallurgy method is the widely used method for the manufacture of copper-tungsten. The various powder metallurgy processing methods are pressing and sintering, infiltration, coreduction of oxides etc. Production methods for these electrical contact materials depend on the composition ratio. For compounds with 60% or less tungsten, the classical method of mixing the powders, pressing, sintering (generally below the melting point of the copper), and repressing may be used. Materials with 60 to 80% tungsten are generally produced by infiltration, either of loose tungsten powder, or of pressed and sintered tungsten compact[6].

The present study deals with the experimental investigations of the preparation of copper-tungsten composite strips by a powder metallurgy route. Chapter 2 gives a general survey of various powder metallurgy routes for making both copper rich and tungsten rich copper-tungsten strips. Chapter 3 describes the scope and the process outline of the present experimental work. Experimental procedure is described in chapter 4. Results and discussion are presented in chapter 5. Finally, conclusions and suggestions for the future work are given in chapter 6 and chapter 7 respectively.

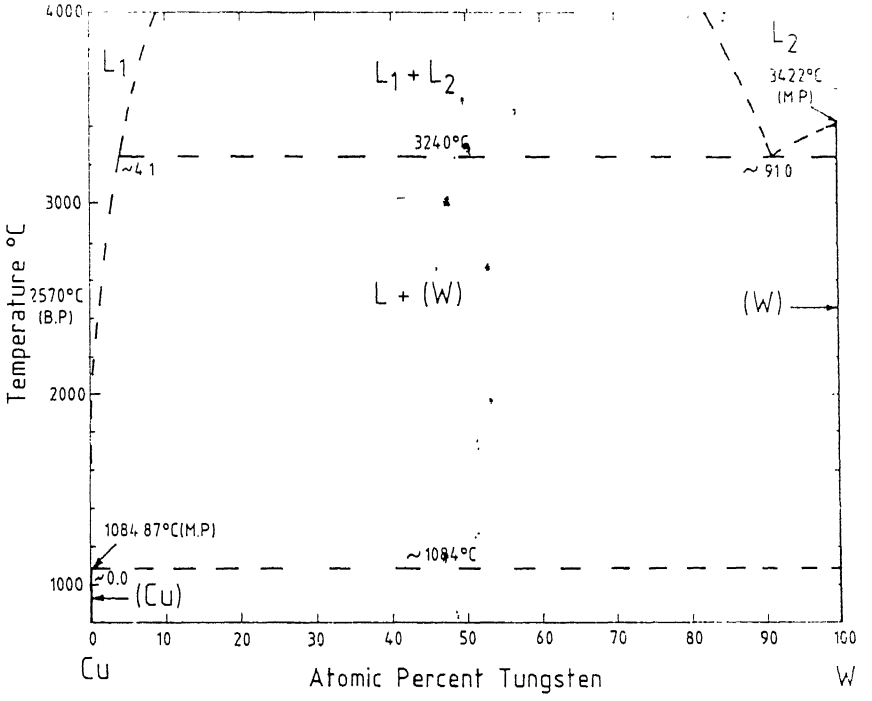

Figure 1.1: Cu-W phase diagram [7]

CHAPTER 2

LITERATURE REVIEW

This chapter reviews various powder metallurgy processing methods for the preparation of copper-tungsten composite materials and the properties such as density, hardness, tensile strength and electrical conductivity of the product produced. The routes used for making copper-tungsten composite materials are pressing-sintering, liquid phase sintering, infiltration, infiltration-mechanical working, co-reduction of mixed oxides-sintering, mechanical alloying-sintering, pressing-sintering-mechanical working and high energy milling-mechanical working.

2.1 Pressing-Sintering Route

In one of the experimental investigations Tousimi et al [8], have prepared 80Cu-20W composites, in which a mixture of 80% copper and 20% tungsten powder were milled together in a vibrating mill under argon gas. The milled powder was then pressed by uniaxial pressing at a pressure of 1600 MPa followed by cold isostatic pressing at 300 MPa. The resulting compacts were subsequently sintered under vacuum at 873K for 3600s. The X-ray diffraction pattern of the compacted copper-tungsten (Fig.2.1) before sintering shows several peaks of the immiscible copper and tungsten. Scanning electron microscope observations were performed on the 80% copper and 20% tungsten compact after sintering, and the microstructures are shown in Figs.2.2a and 2.2b. The compact was found to be homogeneous with a porosity of about 6% (Fig.2.2a). The tungsten lamellar particles (white particles) are homogeneously dispersed in the copper matrix. Their size varies between 0.1μm and 2μm (Fig.2.2b). Tousimi et al [8] have not measured the mechanical properties of the 80Cu-20W composite prepared by the above route. However, they have measured microhardness value, from which they have calculated yield stress of the composite. They have further assumed that due to the strengthened structure of the copper-tungsten composite, the yield stress is nearly equal to its ultimate tensile strength (UTS). In this manner, they have calculated the ultimate tensile strength

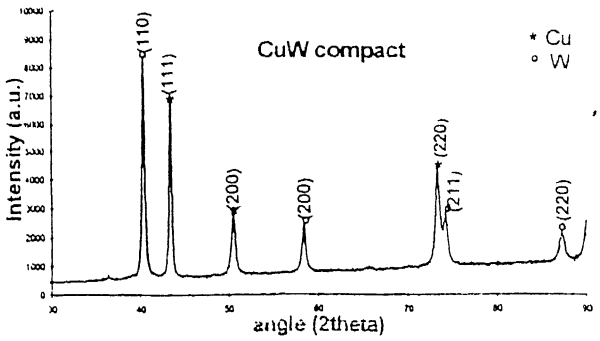

Figure 2.1: X-ray diffraction pattern pressed Cu-W compact showing peaks of the immiscible Cu & W [9]

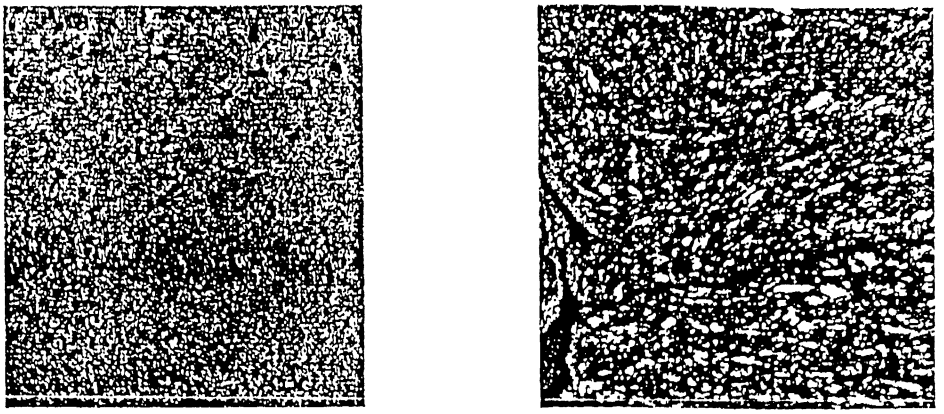

Figure 2.2a(left) & 2.2b(right): SEM micrographs of sintered 80Cu-20W compact at different magnification showing the structure of sample & W dispersion in the Cu matrix [10]

of 80Cu-20W composite containing about 6% porosity as 800 MPa. This composite had a conductivity value of 18.7%IACS at 293K [8], as shown in Table 2.1

Fig.2.3 gives the results on ultimate tensile strength versus conductivity of copper alloys. Tousimi et al have reported from the above figure that copper – tungsten compact prepared for these has rather good mechanical properties but a low conductivity. According to the authors, the low value of electrical conductivity is related to its relatively high porosity. They have proposed that sintering the copper-tungsten compact at higher temperature and pressure for reducing the porosity without increasing the particle grain size could result in a composite with improved mechanical and electrical properties. One of the serious drawbacks of the above study is that the reported value of ultimate tensile strength of the copper-tungsten composite was not measured one, but calculated one. It appears that the reported UTS value is on higher side. It needs further investigations.

Table 2.1 Physical & mechanical properties of Cu-W composite

Calculated UTS	800 MPa
Resistivity at 293K	9.2 μΩ cm
Conductivity at 293K	19.7 % IACS

2.2 Liquid Phase Sintering Route

Liquid phase sintering results in high degree of densification. The various requirements for liquid phase sintering are partial solubility of the solid in the liquid, smaller contact angle and appreciable amount of liquid (35% by volume) for complete densification. The phenomenological aspects of sintering in presence of liquid phase has been discussed by various authors[11][12][13][14].

In one of the experimental work [15], Brush Wellman has prepared copper-tungsten composite by mixing and milling of the elemental copper and tungsten powder.

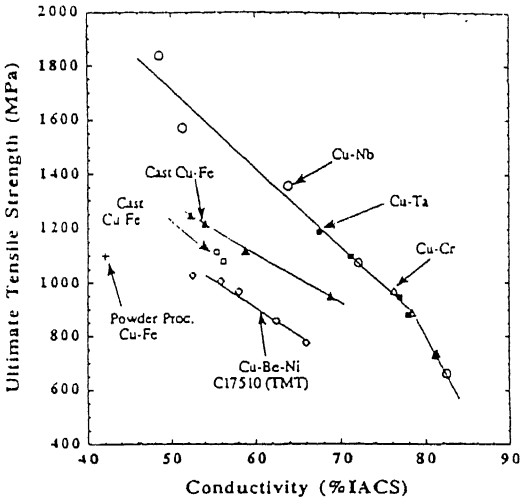

Figure 2.3: Ultimate tensile strength versus conductivity [16]

Typically, the median particle size is about 1-3 μm. After the solids are ground in the aqueous medium in the presence of an organic dispersant, an organic binder is added before the powder agglomeration in a hot air spray dryer takes place. The most important characteristics of the spray-dried powder are good flowability, consistent particle size distribution and density, and homogeneous chemical composition. The powder is compacted into green parts using conventional uniaxial mechanical or hydraulic presses at 138-175 MPa. After forming, the parts are sintered in a hydrogen environment. Depending upon the tungsten content, temperature may be in between 1423-1723K. The microstructures obtained for copper-tungsten composites prepared using infiltration method and this method is shown in Figure 2.4. A more homogeneous phase distribution throughout the body is obtained with this route. The formation of copper pools is apparent in the infiltrated material. The better homogeneity found in powder metallurgy product ensures isotropic behavior for the composite, resulting in uniform thermal conductivity and uniform thermal expansion properties throughout the body. Figure 2.5 shows the thermal expansion of 10% copper and 90% tungsten by weight compared with that of beryllia ceramics up to 1173K. It can be concluded that the thermal expansion match between the copper-tungsten and the beryllia ceramics is appropriate up to 573K.

Sebastian and Tendolkar[17] have made a study in which they have compared the effect of the nature of the starting copper and tungsten powder on the copper-tungsten composites obtained by liquid phase sintering route. In their study two composites A and B were proceed, as follows:

A: Mechanical mixtures of elemental copper and tungsten powders (69W-31Cu)→ compaction→ sintering→ repressing→ resintering

B: Reduction of mixed copper oxide and tungsten oxide→ mixed Cu-W powder (68.5W-31.5Cu) → compaction→ sintering

Figure 2.4: SEM photos of the microstructure of Cu-W composites produced by infiltration (left) & LPS route (right) [18]

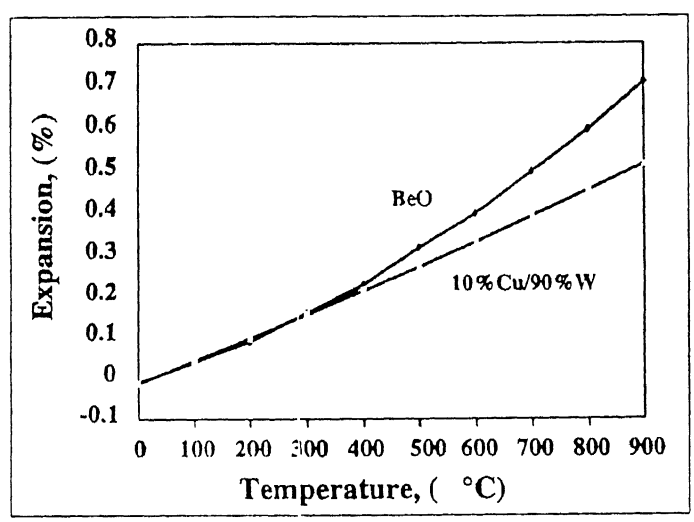

Figure 2.5: Thermal expansion vs temperature for BeO & 90W-10Cu [19]

Composite A and B were sintered at 1423 K, 1523 K, 1573 K and 1673 K for different periods of time. Densification data expressed in terms of "Densification Parameter" as a function of sintering temperature and time for composites A and B are plotted in Figures 2.6, 2.7 and 2.8. It is evident that densification is poor in composite A compared with high densification achieved in co-reduced samples. For constant volume and angle of contact, the interparticle force decreases as the interparticle distance increases. This explains the poor densification obtained in composite A. The tungsten particles in close contact due to segregation are held together by the attractive forces between them and the capillary pressure in the liquid fails to counteract these forces. In composite B, however, excellent dispersion is achieved which enables the particles to be sufficiently apart so that the attractive forces between the particles are reduced. The capillary pressure overcomes this force allowing the liquid to flow freely.though the volume of liquid in composite B, which remains nearly the same as that in composite A.

Sebastian has further reported the results of copper-tungsten composites prepared by the following routes:

A: mixing of elemental powder→ pressing→ sintering→ repressing→resintering

B: mixed oxides of copper and tungsten oxides→ 50Cu-50W mixed powder→ pressing→ sintering

C: pressing of tungsten powder→ sintering→ infiltration of copper with tungsten skeleton

Figure 2.9 gives the variation of the hardness with the volume % tungsten for the copper-tungsten strips produced by the above A, B and C routes[20]. Composites A, B and C were prepared by pressing-sintering, co-reduction of mixed powder and infiltration method respectively. It is evident from this figure that samples prepared from co-reduced oxide powders (i.e. route B) have higher hardness than composites prepared by routes A

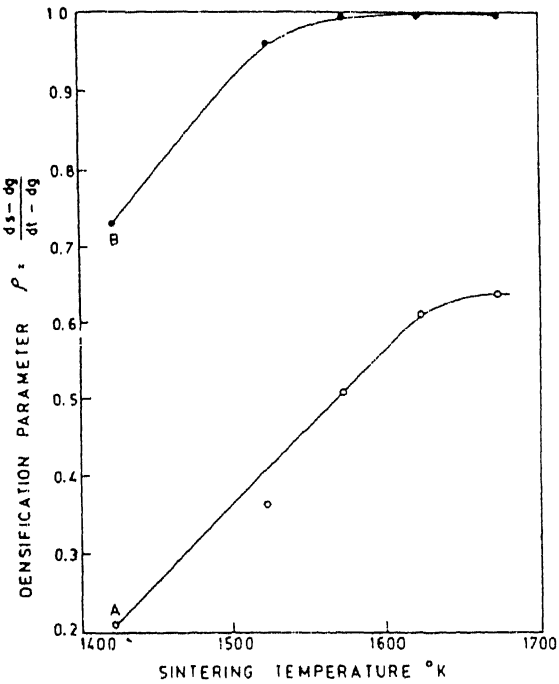

Figure 2.6: Densification parameter as a function of sintering temperature for composites produced from route A & B [21]

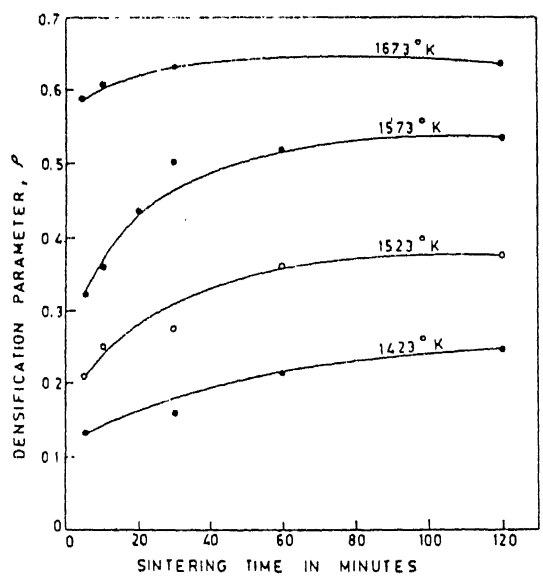

Figure 2.7: Densification parameter as a function of sintering time for mixed W-Cu composite produced from route A [21]

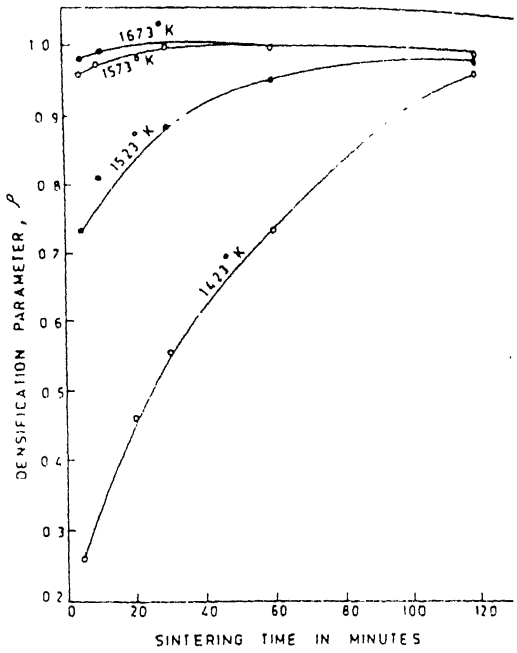

Figure 2.8: Densification parameter as a function of sintering time for composite produced from route B [21]

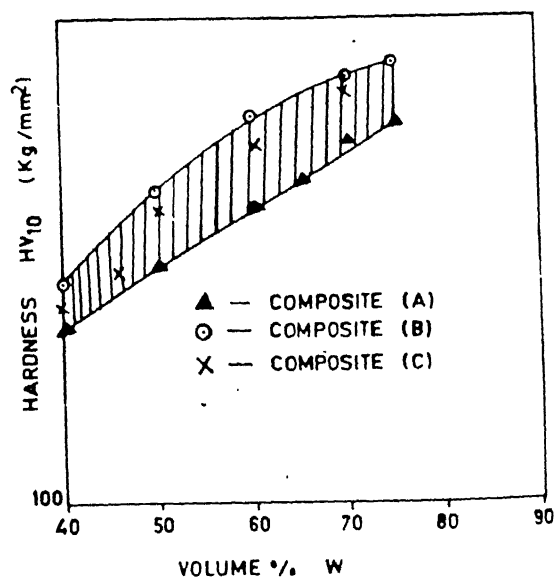

Figure 2.9: Hardness as a function of W content for composites produced from route A, B & C [22]

and C. This can be attributed to the improved dispersion of tungsten in copper as well as the fine and homogeneous microstructures.

Table 2.2 gives the properties of 50Cu-50W composites produced by routes A, B and C containing 50:50 volume % tungsten-copper composites.

Table 2.2 Properties of 50:50 volume % Cu-W composites produced by routes A, B & C.

Processing route adopted	Density %T.D.	Electrical conductivity %IACS	Hardness VPS
(A)	97.98	41.0	195-202
(B)	98.99	45.5	235-238
(C)	98.99	46.0	227-232

Transition metal additions have pronounced effect on liquid phase sintering of tungsten-copper compact. It has been found that nickel can be added to improve the mechanical properties of the tungsten-copper alloys. Small amount of cobalt additions can improve the electrical properties of tungsten-copper alloys. These elements[23] result in improved sinterability. The improved sinterability has been attributed to the beneficial effect of nickel on the wetting between liquid and solid phase. Figure 2.10 shows the effect of the dopant on the sintering of the pure tungsten. In the presence of liquid phase, however, the effect of the activators is rather small as shown in Figures 2.11 and 2.12. For the higher amount of liquid phase (Fig.2.12), beneficial effect of both dopants is negligible. In the case of cobalt, it is known that cobalt has a low solubility in copper and that copper-cobalt alloys show liquid immiscibility. It is therefore possible that cobalt will tend to precipitate at the copper-tungsten interface. In practice it has been found that cobalt addition to copper-tungsten alloys produce the W_6Co_7 phase on the surface of the tungsten grains[24]. It may influence the wetting characteristics. By contrast, nickel forms a complete series of solid solutions with copper, and therefore the nickel additions seems likely to remain in solution in the liquid copper rich phase rather than form an

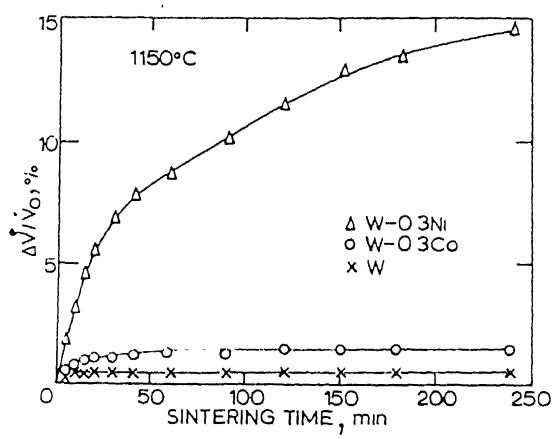

Figure 2.10: Influence of added metals on volume shrinkage (ΔV/Vo) of pure W compact sintered at 1423K in hydrogen atmosphere [25]

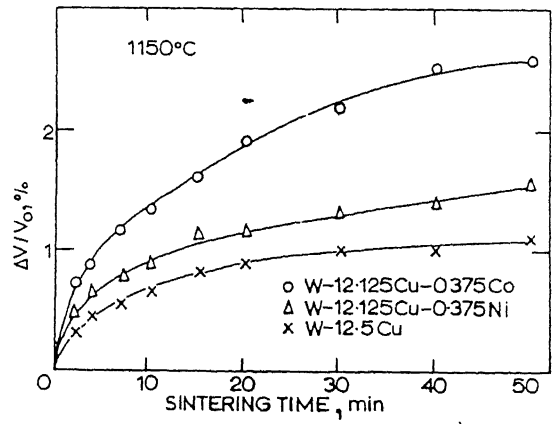

Figure 2.11: Influence of added metals on volume shrinkage (ΔV/Vo) of W-12.125Cu system, sintered at 1423K in hydrogen atmosphere [25]

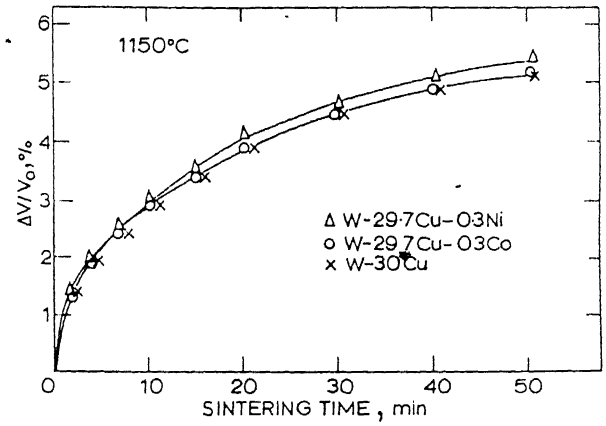

Figure 2.12: Influence of added metals on volume shrinkage (ΔV/Vo) of W-29.7Cu system, sintered at 1423K in hydrogen atmosphere [25]

intermediate compound on the surface of the tungsten particles. Figure 2.12 shows the effect on sintering of increasing the proportion of the liquid phase. The additions of 0.3% cobalt or nickel have negligible effect on the densification of W-29.7% Cu alloy. This is consistent with the view that if the liquid phase were to exceed 35 vol.-% then complete densification of the compact by particle rearrangement might be possible[26]. This is supported by the results of Eremenko et al[27], which showed that the shrinkage increased five fold as the copper content was increased from 20-50%. It was concluded that in high copper alloys the particle rearrangement mechanism dominated because of the large fraction of liquid present, and that any effect of additions of activating agents would tend to be obscured.

2.3 Infiltration Method

Infiltration consists of placing a compact or a piece of solid metal in the furnace that will melt during sintering on or below the porous green compact to be infiltrated. Once the material is melted it will be drawn into the interconnected porosity by capillary action if there is sufficient wetting between the two[28]. Comparison of properties of copper-tungsten prepared from pressing-sintering route and infiltration route has already been shown in Fig. 2.9 and Table 2.2. Densities obtained by infiltration technique are shown in Figure 2.13. The designations A, B and C have the same meaning as explained earlier in section 2.2. It can be seen that the density of the composites obtained from the infiltration route is higher as compared to that obtained from liquid phase sintering of copper-tungsten compacts prepared from elemental powders. However it is similar to that obtained by liquid phase sintering of copper-tungsten compacts prepared from the mixed powder obtained from the reduction of mixed tungsten oxide-copper oxide.

Complete densification by liquid metal infiltration may be impossible because of the presence of fine porosity within the original particles of the green compact and the presence of closed porosity in the compact.

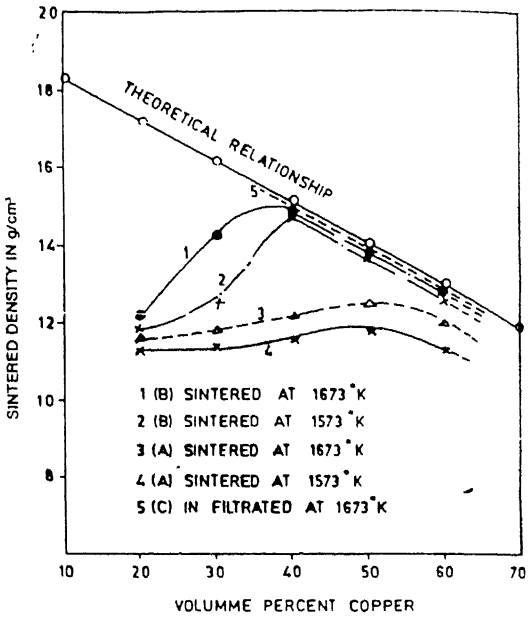

Figure 2.13: Sintered density as function of volume percent copper for composite produced from route C [22]

2.4 Infiltration-Mechanical Working Route

Binary composites of tungsten and copper provide a useful model in the study of the deformation of heavy metals, as there is no mutual solubility in either the solid or liquid state. This is in contrast to commercial heavy metals, which contain such alloying elements as nickel or iron[29]. The composites were made by liquid infiltration of tungsten powder preforms by copper. After sintering, the typical diameter of the tungsten particles was around 20μm. The copper-tungsten composites with 10wt%, 20wt%, 30wt% and 40wt% of copper were used for the experimental work. The materials were cold rolled. The total reduction was in the range of 10-50%. Annealing was carried out for 3600s in air on materials that had been cold worked by 25%. Hardness testing of the composites was carried out using a 2 mm diameter ball and a load of 120 kg. Tensile testing was performed on sheet specimens, 1.25 mm thick, with a gauge length of 20 mm and width of 5 mm.

Figure 2.14a shows the increase in hardness as a function of increased cold working and Figure 2.14b shows how the tensile strength of the composites increases with the increasing cold working. The authors have not reported as to how the % elongation values of the tungsten-copper composite changed with percent cold working deformation. There is an increase in hardness and increase in tensile strength as the proportion of the harder and stronger tungsten phase increases. Annealing reduces the hardness of the composite (Fig.2.15) provided that the temperature is above 623K. When the composite is deformed by up to 50% there is no sign of macroscopic elongation of the tungsten particles (Figs.2.16a and 2.16b), but at around 90% reduction in thickness, the tungsten particles (Fig.2.16c) are being seen elongated in the direction of rolling. When the deformation of a two-phase aggregate containing a soft matrix and a hard reinforcement is analyzed, there are two extremes forms of deformation possible. The first is when the strain in each of the components is equal, while the second is when the strain is concentrated in the soft matrix, leaving the hard particles essentially undeformed. In tungsten-copper composite, if the first model were to be appropriate, then the specimen cold rolled and subsequently annealed at 723K will be harder than the unrolled

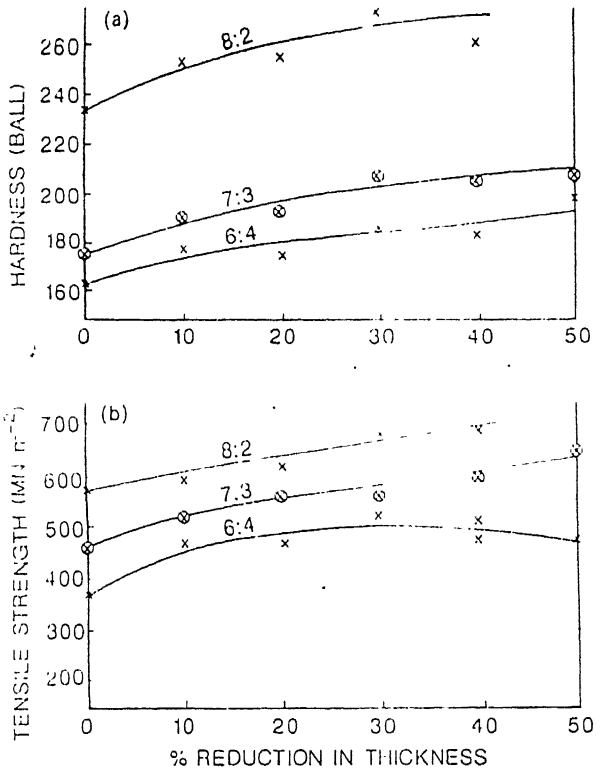

Figure 2.14: Effect of cold work on hardness & tensile strength of W-Cu composites (the ratio shows W:Cu ratio) [30]

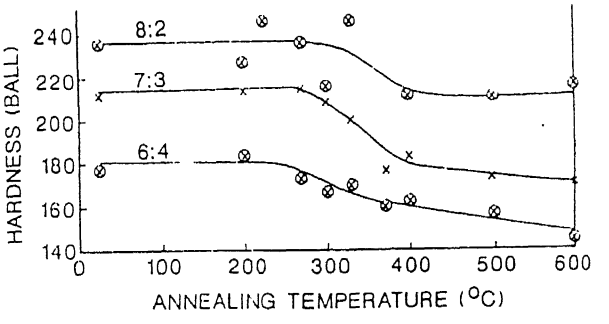

Figure 2.15: Effect of annealing on hardness of W-Cu composites cold worked by 25% (the ratio shows W:Cu ratio) [30]

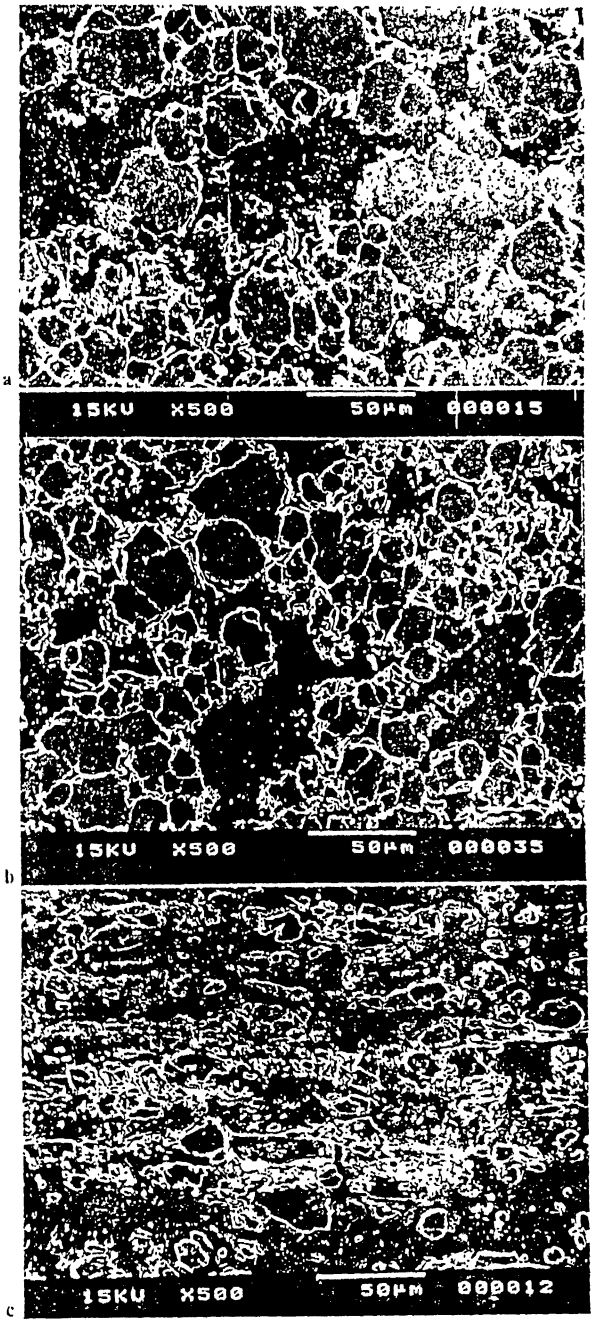

a 0%; *b* 25%, *c* 90%

Figure 2.16: Effect of given amount of cold work on microstructure of 58.1W-41.9Cu composite [31]

composite. This is because recrystalliztion in the tungsten will not have started at the annealing temperature, leaving the tungsten particles cold worked, and therefore harder, after annealing. Additionally, there will be evidence of elongation of the tungsten particles after cold working. Neither of these predictions is true. A comparison of Figures 2.14a and 2.15 shows that the increase in hardness due to cold working is eliminated following annealing at 723K, while metallographic examination shows that there is no sign of macroscopic elongation of the tungsten grains at up to 50% cold working. According to the theory that deformation is confined to the softer copper phase, the structure after annealing should be approximately of the same hardness as the cast material, while the tungsten particles should remain equiaxed after deformation. This appears true from the Figures 2.14a and 2.15. If the annealing curves of Figure 2.15 are considered, it can be seen that the recrystallization temperature of the copper matrix of the composite decreases slightly as the copper content of the composite decreases. This can be explained if the amount of deformation in the copper is assumed to increase with increasing tungsten content, as shown in Table 2.3, since the recrysatallization temperature will decrease slightly with increasing amounts of cold working.

Table 2.3 Increase in % deformation with increase in tungsten content.

Composition, wt%	Deformation in copper phase, %
60W-40Cu	41.1
70W-30Cu	50.5
80W-20Cu	73.5

If the working of these composites to produce practical shapes at temperature above room temperature is considered, it is clear from the above that for moderate deformations, the deformations will be confined to the copper and there will be no advantage in working at 1223K, rather than at 723K. This is because, for both temperatures, there will be hot working of the copper matrix and no deformation of the tungsten particles. Since it is not possible to recrystallise the tungsten particles at temperatures blow the melting point of the copper, this suggests that the formation of

components should be carried out in a multistage process, with the deformation of the component in each stage being restricted to such a value as to confine the deformation to the softer copper phase.

2.5 Co-reduction cum Sintering of mixed Copper oxide and Tungsten oxide Route

The chromium-zirconium, copper-chromium and copper- aluminum oxide alloys are well known for their high hardness and high electrical conductivity, which cannot be obtained in common copper alloys. In the Cu-Cr and Cu-Zr alloy which are manufactured by precipitation hardening process, the precipitated chromium or zirconium phase dissolve in copper matrix at high temperature and then this causes the decreasing hardness. In the copper-aluminum oxide alloy, which is manufactured by internal oxidation process, the aluminum oxide particles do not dissolve in copper matrix even at high temperature and then hardness does not decrease. But, the electrical conductivity is less than 80% IACS, because aluminum cannot be completely oxidized by internal oxidation method. Tungsten is well known for its very little solubility into copper and very high melting point. But, it is very difficult to obtain the fine tungsten particles and their uniform dispersion. Therefore, co-reduction method of tungsten trioxide and copper oxide powder was applied to develop the fine tungsten dispersed copper alloy. In this method[32], tungsten trioxide and copper oxide powders were mixed by attrition mill followed by co-reduction in hydrogen atmosphere, at 573K, 773K and 973K. When these oxides were completely reduced to the metal, copper-10mass% tungsten alloy powder was obtained. Co-reduced powders were hot pressed under a pressure of 20 MPa at 1173K. Scanning electron microscope photographs of raw oxide powders are shown in Figure 2.17. The shape of copper oxide powder was almost globular. Figure 2.18 shows microstructures of copper-10 mass% tungsten alloy hot pressed at 1173K. Pores were hardly observed as shown in Fig 2.18a. According to the scanning electron microscope observation (Fig2.18b) fine white tungsten particles were uniformly distributed. When mixed powder was reduced, copper oxide was easily reduced to the metallic copper at 573K, however tungsten trioxide was not reduced completely even at 773K. A part of tungsten was reduced to the tungsten dioxide at 773K. Tungsten trioxide was completely

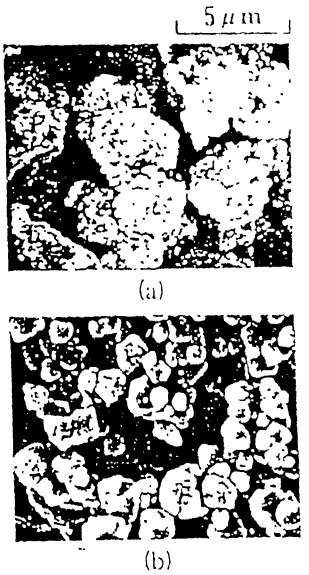

Figure 2.17: SEM photographs of raw oxide powders [33]

(a) Tungsten-trioxide powder

(b) Copper oxide powder

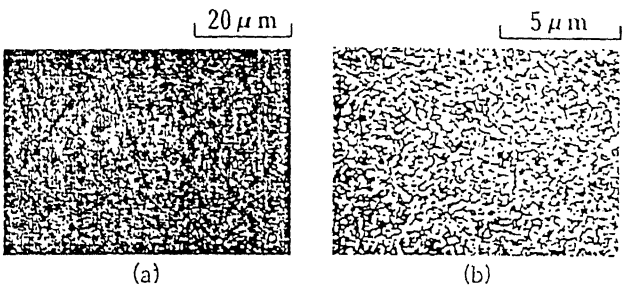

Figure 2.18: Microstructures of sintered 90Cu-10W obtained by the powder reduced at 973K [33]

(a) Optical microstructure

(b) SEM microstructure

reduced to the metallic tungsten at 973K. From these results, the reduction temperature of 973K is suitable for getting this co-reduced powder. Table 2.4 shows some physical properties of the hot pressed copper-10mass% tungsten alloy. The density of this alloy was 99% of the theoretical. This hot pressed alloy had both higher hardness and higher electrical conductivity at the room temperature than those of commercially available copper-zirconium alloy. Figure 2.19 shows the effects of testing temperature on the hardness of the hot pressed alloy. The hardness of this alloy is higher than that of copper-zirconium alloy at each temperature. Figure 2.20 shows the hardness affected by annealing temperature. Above 673K of annealing temperature, the hardness of the copper-zirconium alloy decrease remarkably with the increase in the temperature. But, the hardness of the hot pressed copper-10mass%tungsten alloy did not decrease even after annealing at 1073K. Since dispersed tungsten particles and copper matrix are not mutually solid soluble from room temperature to high temperature, these tungsten particles can strengthen the copper matrix even at high temperature. On the other hand, incase of copper-chromium alloy, the precipitated zirconium easily dissolves in copper matrix at high temperature. So, precipitated particles cannot strengthen the copper matrix any more.

Table 2.4 Physical properties of sintered Cu-10mass%W alloy after annealing.

Relative density, %	99
Hardness, $H_{v0.3}$	147
Electrical conductivity, %IACS	84

In one of the experimental work[34], the nanocomposite tungsten-copper powders were prepared by ball milling and co-reduction of oxide powders. This nanocomposite tungsten-copper powder was used for metal injection molding. The micro-homogeneous tungsten-copper nanocomposite powders were prepared by mixing and ball milling of tungsten trioxide and copper oxide powder, and co-reduction of these ball milled oxide powders. The authors have not reported the temperature at which co-reduction of these oxides powders were carried out.

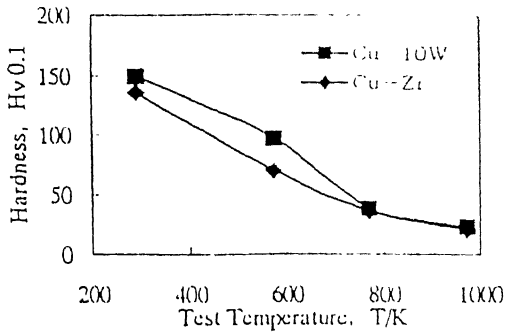

Figure 2.19: Effects of testing temperature on the hardness of the 90Cu-10W sintered alloy [35]

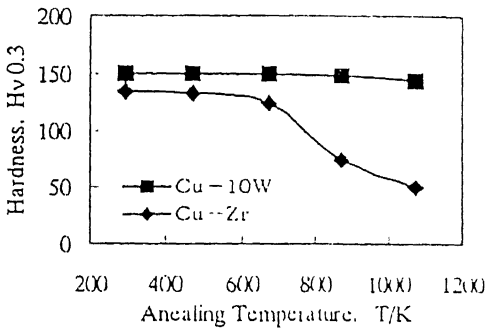

Figure 2.20: Effects of annealing temperature on the hardness of the 90Cu-10W sintered alloy [35]

Figure 2.21 shows the morphology of 80W-20Cu powders prepared by this method. As shown in these micrographs, individual tungsten powders of particle size of 30-70 nm were homogeneously mixed with a binder like copper phase, forming an aggregate of tungsten and copper. The particle size of the agglomerated tungsten-copper composite powders was about 10 μm. The metal injection molding feedstocks were sintered at temperature between 1323K and 1623K in a pure hydrogen atmosphere for 7200s. Figure 2.22 shows the dependence of sintered density of tungsten-copper metal injection molding specimens on these sintering temperatures. The specimens sintered for 7200s at 1323K had a relative density of only 61%. However, raising the sintering temperature increased the sintered density. The relative density of the sintered part was increased to more than 95% by sintering at 1423K, and the specimen sintered at 1623K had a relative density of 98.5%. The rapid increase in the sintered density in that temperature range can be attributed to the change of the sintering mechanism from solid to liquid phase sintering. Figure 2.23 shows the scanning electron microscope micrographs of the tungsten-copper specimens sintered at 1623K for 7200s. As shown in these micrographs, the tungsten grains are distributed homogenously in the copper matrix. However, the average size of the tungsten grains increased to about 1.5μm from an initial size of about 50 nm.

2.6 Mechanical Alloying of Cu-W Powder-Sintering Route

Mechanical alloying is a high-energy ball milling technique in which mixtures of powders of different metals or alloys / compounds are milled together. Material transfer is involved in this process to obtain a homogeneous alloy[36]. The mixed powder is milled for desired length of time until a steady state is reached when the composition of the every powder particle is the same as the proportion of the elements in the starting powder mix. During high energy milling the powder particles are repeatedly flattened, fractured and rewelded[37]. The force of the impact plastically deforms the powder particles, creates new surfaces, and enables the particles to weld together. With continued deformation, the particles get work hardened and then fracture. Owing to the continued impact of grinding balls, the structure of the particles is steadily refined.

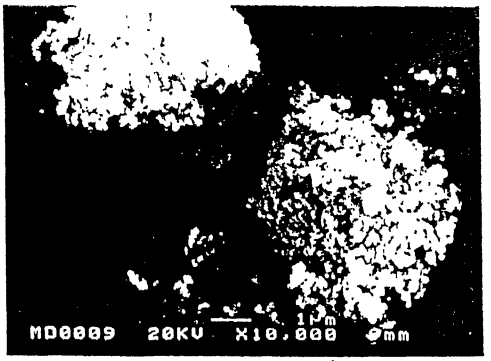

Figure 2.21: Scanning electron micrograph of nanocomposite W-20Cu powder prepared by ball milling and co-reduction of pertinent oxide powders [38]

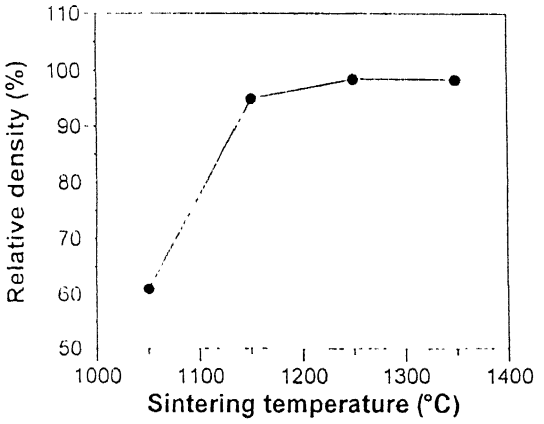

Figure 2.22: Dependence of sintered density of W-Cu MIM specimens on sintering temperature (sintering time 7200s) [38]

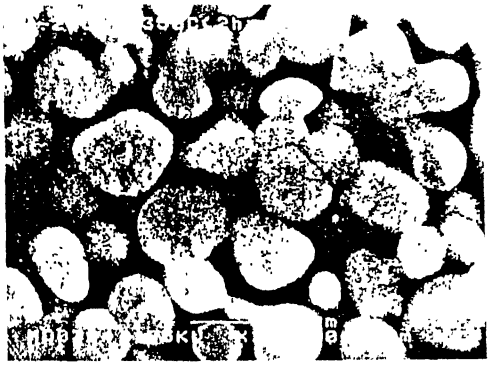

Figure 2.23: Scanning electron micrograph of W-20Cu specimen sintered at 1623K for 7200s [38]

The nanosize crystalline structure of the copper-tungsten composite was prepared by mechanical alloying of the elemental copper and tungsten powder in an attritor mill[34]. Tungsten powder with a mean particle size of 4.2 μm and a purity of 99.9%, and commercial grade atomized copper powders of irregular shape with a mean particles size of 50.42μm and purity greater than 99.5%, were used as raw elemental powders. The copper and tungsten powder mixes of compositions equivalent to 80w-20Cu and 70W-30Cu were mechanical alloyed in a stainless steel ball charged, high energy attritor for milling times up to 360000s under a protective argon atmosphere. After mechanical alloying for more than 180000s, the mechanical alloyed copper-tungsten powder reached the steady state stage[39], in which the powder morphology was characterized by an equiaxed shape with a mean particle size of 3.2μm. At this stage, the copper peak completely disappeared from the X-ray diffraction pattern of the 80W-20Cu specimens suggesting that the copper does not exist as a separate phase in tungsten, even though this copper content is above the solubility limit in tungsten determined by the solubility analysis. Figure 2.24 shows the morphology of this mechanical alloyed composite powder. This mechanical alloyed powder was cold pressed into disc shaped compact with a relative density of 40%. The sintering of the compacts was carried out in the temperature range of 1273K-1623K for 3600s in hydrogen atmosphere. Figure 2.25 shows the sintered density of the mechanically alloyed 80W-20Cu specimens as a function of sintering time at a temperature of 1373K. The mechanical alloyed specimens had shown a higher sintered density, having a density greater than 91% after sintering for only 60s, than copper-tungsten specimens mixed without ball milling. The mechanical alloyed specimens reached a relative sintered density of 96% on sintering at 1373K for 3600s, while the simply mixed copper-tungsten specimens had a relative sintered density of only 73% following the same sintering treatment. The sintering behavior of the mechanical alloyed 70W-30Cu specimens was similar to that of the mechanical alloyed 80W-20Cu, except that its sintered density was higher than that of the later. The mechanical alloyed 70W-30Cu specimens were densified to a relative density greater than 98% by sintering at 1373K for 3600s. The enhanced sinterability of the mechanical alloyed copper-tungsten powder compact might be attributed to several effects: the effect of activated sintering of the impurity metal introduced by the mechanical alloying

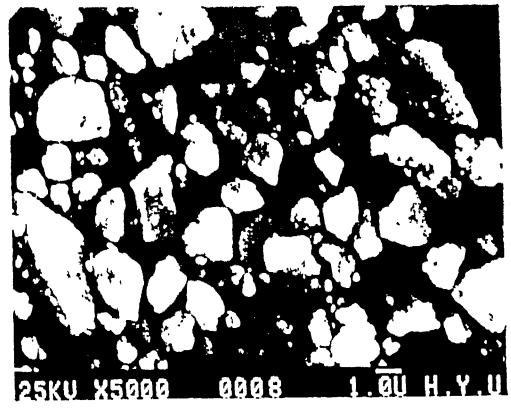

Figure 2.24: Scanning electron micrograph of mechanically alloyed W-Cu composite powder [40]

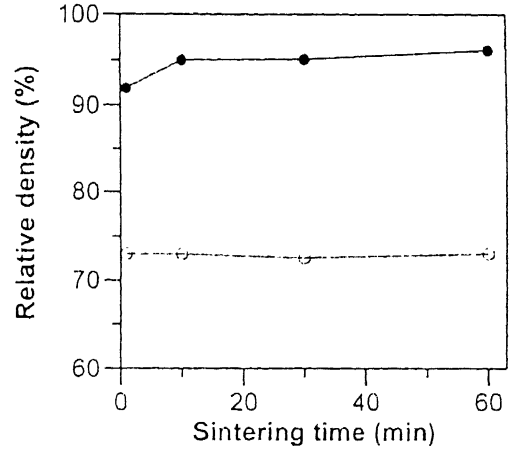

• mechanical alloyed; o simply mixed

Figure 2.25: Sintered density as function of sintering time for 80W-20Cu specimens sintered at 1373 in hydrogen atmosphere [40]

process[41], a thermal effect related to the transformation of the severely strained mechanical alloyed crystalline structure, and finally, to the intrinsic homogeneous, ultra fine structure of the mechanical alloyed composite powder. The high sinterability of the mechanical alloyed copper-tungsten system seems to be a result of the unique characteristic of the nanocrystalline composite structure of the mechanical alloyed copper-tungsten alloy, with its fine, homogeneous mixed state of nanosize copper and tungsten phase, as well as a crystalline structure with high strain energy owing to severe cold working.

The formation of a continuous network of liquid copper phase can enable a high degree of particle rearrangement without forming pores or a liquid pool in the copper-tungsten system, which is characterized by low wettability[42]. The recrystallization of the severely strained tungsten crystallites in the mechanical alloyed copper-tungsten powder seems to take place at a low temperature of about 1023K, according to differential scanning calorimetry. Such a transformation of the tungsten crystal structure in the mechanical alloyed copper-tungsten powder, along with the thermal energy released by this transformation, might also contribute to the higher sinterability of the mechanical alloyed copper-tungsten powders. The sintering of the nanostructured copper-tungsten composite powder was characterized by the low temperature sintering of the nanosize tungsten crystallites presented in the individual mechanical alloyed copper-tungsten powder. The sinterability of these nanosize tungsten crystallites was so high that they were able to form a newly sintered structure even on sintering below 1173K. Such sintering of inner nanostructred tungsten crystallites in mechanical alloyed copper-tungsten powder seems to contribute to the enhanced sintering of the mechanical alloyed copper-tungsten powder.

2.7 Pressing-Sintering-Mechanical Working Route

Copper-tungsten composite materials containing greater than 50% of tungsten are manufactured by liquid phase sintering of the copper and tungsten powders [43], or by infiltration of a tungsten skeleton with liquid copper[44]. Copper-tungsten composite

Figure 2.26: High energy milled Cu-8 vol.-%W composite powder [47]

(a) Particle shape

(b) Particle structure

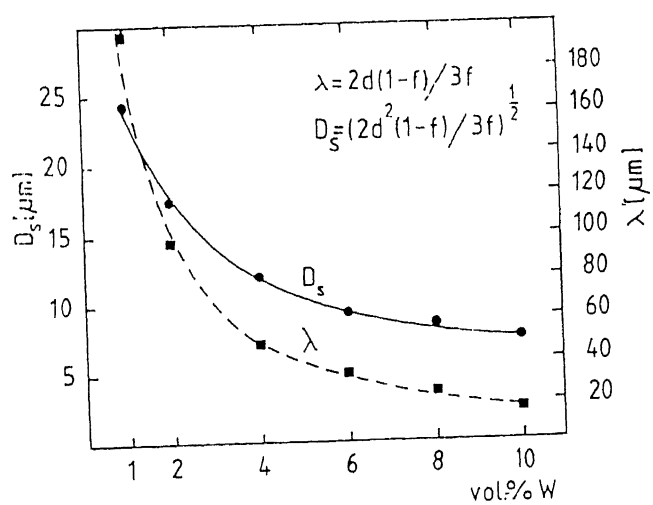

Figure 2.27: Theoretical mean paths λ & interparticle spacing D_s of Cu-W composite materials [47]

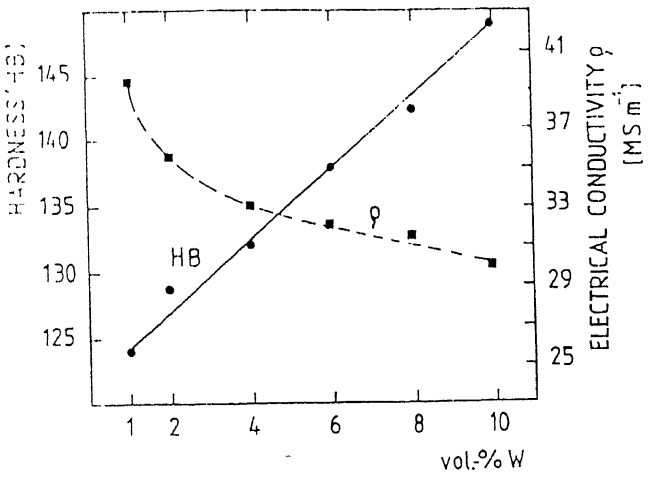

Figure 2.28: Hardness (HB) & electrical conductivity of cold extruded Cu-W composite materials [47]

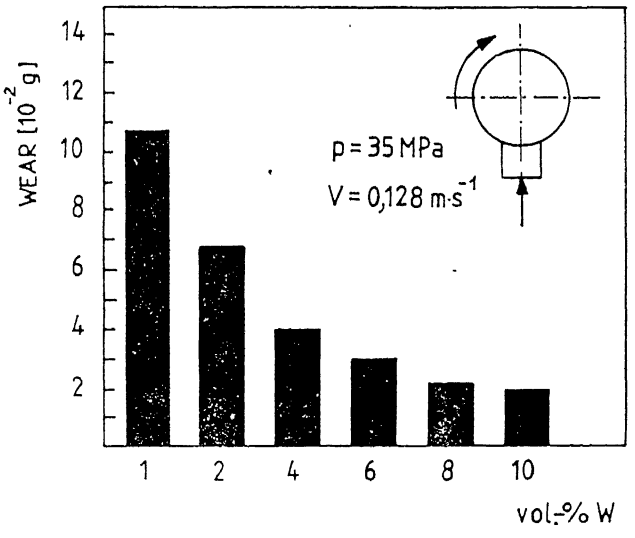

Figure 2.29: Abrasion resistance of cold extruded Cu-W composite materials [48]

annealed in air either at 573K or 773K for 1800s, 3600s, 7200s, 14400s, and 28800s in order to determine the influence of annealing on the hardness and electrical conductivity (Figs.2.30 & 2.31). Cold pressing followed by sintering of the copper-tungsten composite powders produces relative densities of less than 80 %. Due to high hardness of tungsten compared to copper, tungsten particles on the surface and within the copper particles decreases the plasticity of copper-tungsten composite particles and increases friction between particles. This results in relatively low green densities. During sintering of copper-tungsten composites, tungsten particles on the surface of the composite powders hinder copper neck formation and hence shrinkage. Cold direct extrusion of copper-tungsten sintered billets produces a high densification. Pores are flattened due to the compressive stresses and the opposite walls of the pores can approach each other. In the case of extruded sintered materials, which do not contain dispersed particles, the opposite walls of pores cold-weld dividing the pores into a chain of very small pores. Composite sintered materials contain dispersed particles within the matrix and on the surface of the pores and prevent welding of the opposite walls of the pores as shown in Figure 2.32. The highest hardness after extrusion was obtained by 10 vol.-%W. The main factors influencing hardness are strain hardening and interparticle spacing. Electrical conductivity is influenced more on the mean free path (vol.-%W) than on porosity. Annealing of extruded materials at 573K and 773K results in the rapid decrease of hardness due to recrystallisation. Recrystallisation process is practically completed after 3600s of annealing at 573K as indicated by hardness measurements. Negligible grain growth was observed during prolonged annealing. This is due to the retarding influence of tungsten particles. Although tungsten particles do not stop recrystallisation, they inhibit grain growth. The maximum electrical conductivity after annealing was obtained in the Cu-1 vol.-% W composite material.

2.8 A new method for making Cu-W composite strip: Slurry Casting-Hot Rolling Process

Another possible method for making copper-tungsten composite material could be to mix copper powder and tungsten powder in a high-energy ball mill. A coherent and

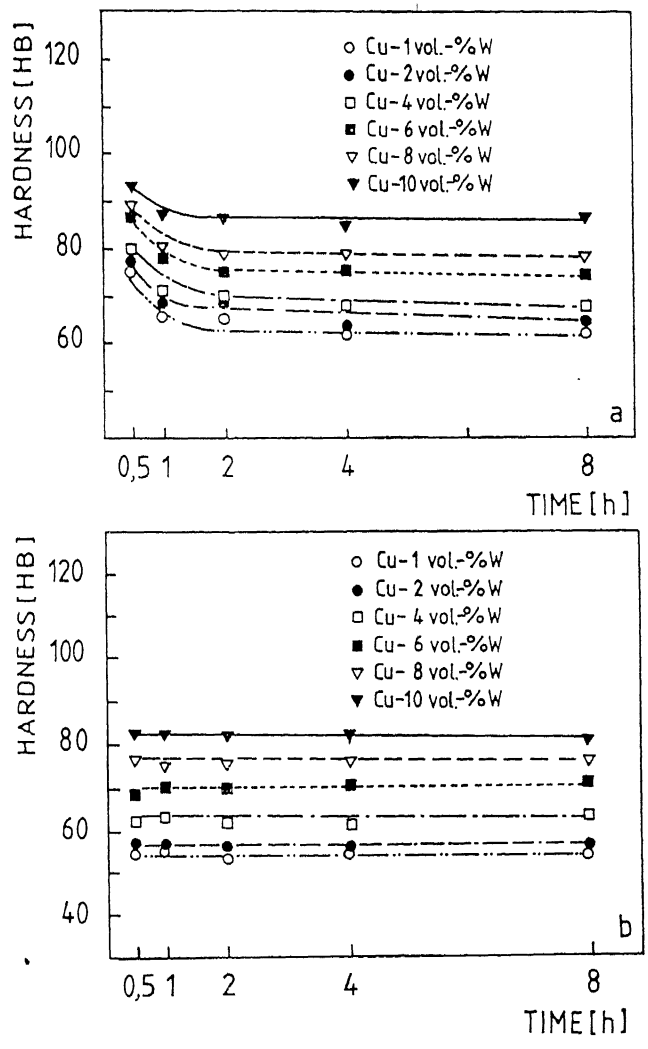

Figure 2.30: Hardness (HB) of cold extruded Cu-W composite materials after annealing during different times- a) at 573K b) at 773K [48]

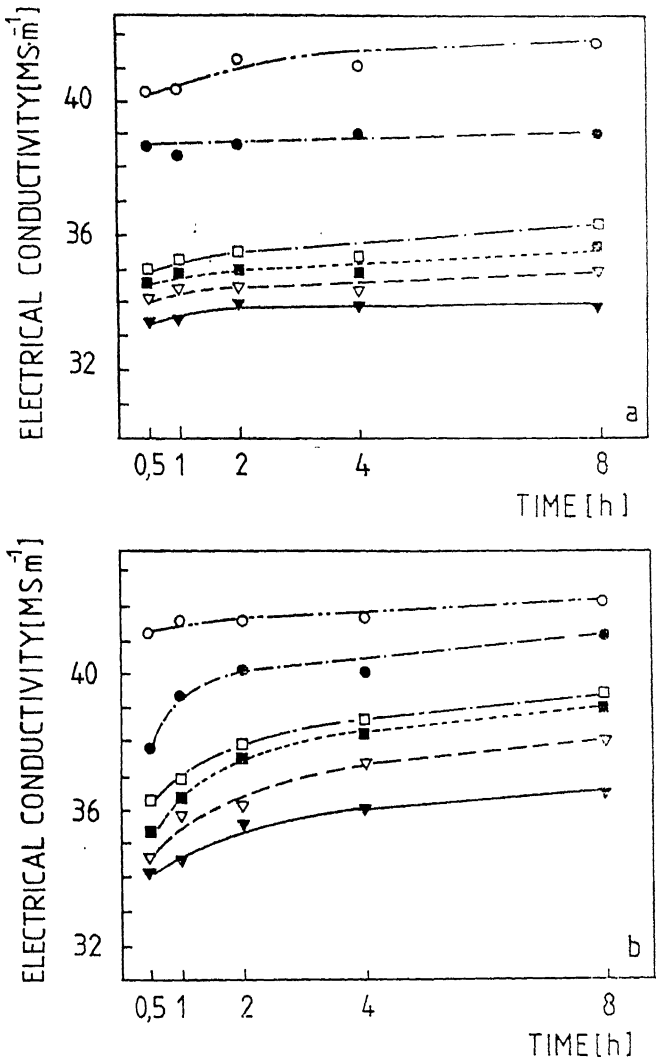

Figure 2.31: Electrical conductivity of cold extruded Cu-W composite materials after annealing during different times- a) at 573K b) at 773K (symbols similar to Figure 2.30) [48]

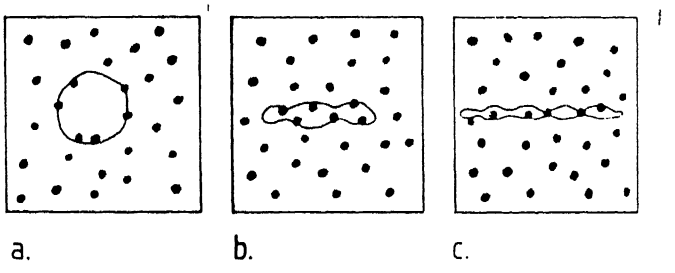

Figure 2.32: Closing up of a pore in the composite material during cold plastic extrusion [49]

(a) Pore shape after sintering

(b) Pore shape after medium deformation

(c) Pore shape after high deformation

flexible "green" copper-tungsten composite strip can be prepared by slurry casting process[50]. It is also known as slip casting[51]. High-energy mill powder mixture is mixed with a suitable liquid binder, which produces homogeneous and free flowing slurry. The slurry is cast into a strip form in a suitable mould, which is subsequently dried to prepare a coherent and flexible strip. The choice of binder is an important factor. It should be such that it does not leave behind undesirable impurities after sintering process. Methyl cellulose, various types of resins, etc are most commonly used binder for this purpose. Further, the binder should be such that it produces homogeneous and free flowing slurry, when mixed along with metal powder in a suitable vehicle, even at low concentration. The most commonly used vehicle for methyl cellulose binder is water.

The dried "green" copper-tungsten strips can be sintered at 1273K in hydrogen for a suitable period of time. The reducing atmosphere during sintering removes undesirable impurities, e.g. surface oxide films, from the surface of copper or tungsten particles. This reducing atmosphere also protects the green strips from oxidation. The sintered strip is then subjected to hot rolling under protective atmosphere, which would result in the densification of the sintered Copper-Tungsten strip. The various steps used in this method are given in Figure 2.33 in the form of flow chart.

The advantages offered by this proposed route for making copper-tungsten composite material is that it uses hot rolling process for densification, which can produce copper-tungsten composite in thin strip form on a continuous basis. It can be noted that the earlier discussed conventional powder metallurgy routes based on pressing-sintering, liquid phase sintering, etc are not suitable for making thin copper-tungsten contact materials having complex shapes on a mass production scale. The proposed route has such an advantage.

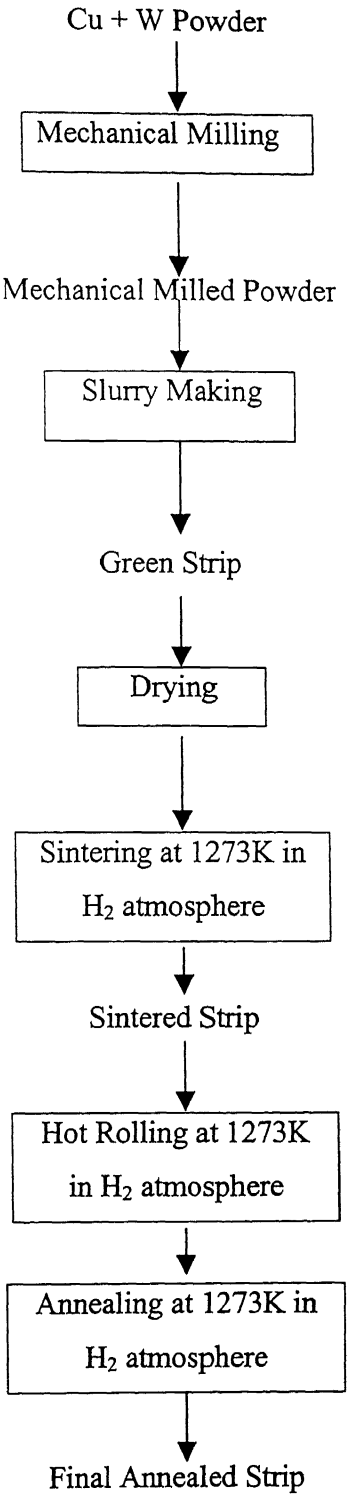

Figure 3.1 Process outline of the present experimental work

CHAPTER 3

EXPERIMENTAL PROCEDURE

3.1 Materials

Copper Powder

Atomized copper powder, supplied by Greenback Industries, Inc., U.S.A. was used for the present experimental work. The particle size distribution of the copper powder is shown in Figure 3.1.

Tungsten Powder

Tungsten powder of grade TMP (2-3) supplied by Electronica Machine Tools Ltd, Nasik was used in the present study. The particle size distribution of tungsten powder is shown in Figure 3.2. It was done in FRITSCH PARTICLE SIZER ANALYSETTE 22.

Binder

Reagent grade anhydrous methylcellulose powder having methoxy content of 28%-32% was used as binder.

Plasticizer

Reagent grade glycerol having density of 1.255-1.266 g/ml at 293 K was used as plasticizer.

Vehicle Medium

Distilled water was used as a vehicle medium for dissolving the binder.

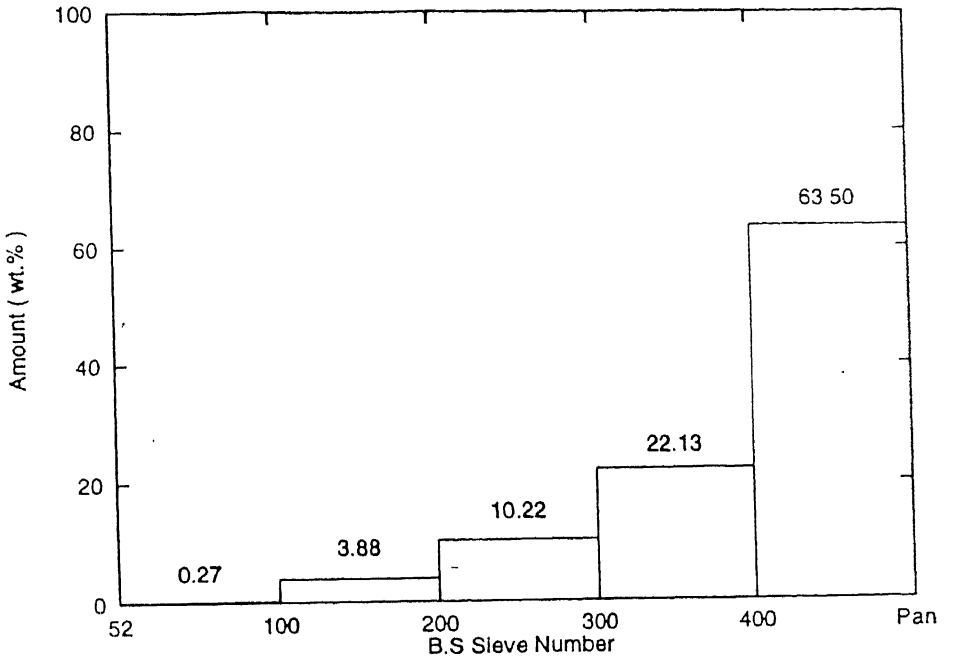

Figure 3.1: Particle size distribution of copper powder

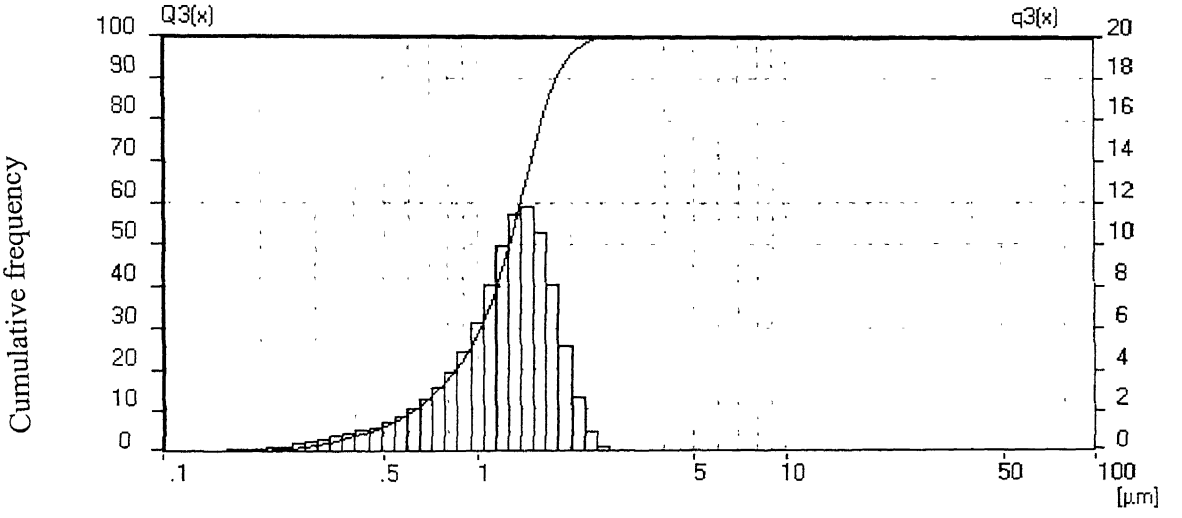

Figure 3.2: Particle size distribution of tungsten powder

Gases

IOLAR-2 grade hydrogen and nitrogen gases were used in the present work.

3.2 Preparation of Cu-W Composite Powder

The copper-tungsten composite powder was prepared by high energy milling of high purity copper and tungsten powder in a high-energy attritor mill. Tungsten carbide balls of diameter 18 mm with weight of 65 gm each were used as the grinding medium. A powder mix of 70:30, 80:20, 90:10, and 95:5 ratios by weight of copper and tungsten powders were separately mechanically milled in wet condition. Acetone was used during grinding. It minimizes cold welding between powder particles and thus minimizes agglomeration. The volume of vial that contained copper-tungsten powders, balls and acetone was 250 cc. The total volume of the material, inside the vial should be one fourth of the volume of the vial for the efficient grinding. The maximum shaft speed was kept 300 r.p.m in the mill. The copper-tungsten powders were milled for a period of 16 hours. The milling was carried out in air. Higher the ratio faster is the grinding.

3.3 Preparation of Green Strips by Slurry Casting Method

Green strips were prepared from high energy milled 95Cu-5W, 90Cu-10W, 80Cu-20W and 70Cu-30W composite powders. The procedure used for all the cases was same.

The copper-tungsten green strips were prepared by using the batch process of slurry casting method. The optimum amount of water, glycerol and methylcellulose taken for slurry is shown in Table 3.1. This composition resulted in the formation of the homogeneous slurry of good flowability. At first a dry mix of binder and metal powder was prepared and then a solution of glycerol in water was made. This was done to prevent the agglomeration occurring during mixing of binder with solvent. Then the premix was mixed with the aqueous solution of glycerol in a beaker with the help of a laboratory stirrer for 900s. Homogeneous slurry having good flow characteristics was

obtained. Mixing by the stirrer and casting of slurry were done carefully to reduce the amount of entrapped air bubbles in the cast strips.

Table 3.1 Composition of slurry

Composition	Weight Percentage (%)
Methyl cellulose	1
Glycerol	5
Water	25
Cu-W powder	69

The green strip was prepared by casting the copper-tungsten slurry into a flat horizontal detachable type mould. Prior to pouring, the inner surface of the mould was coated with oleic acid, which acted as a releasing agent. After pouring, the excess slurry was scrapped off from the mould by a scrapper blade to maintain the uniformity in thickness of green cast strip. The mould was heated from the bottom by placing it on a hot plate. Hot air blast was also provided on the surface of the strip during drying.

3.4 Sintering of the Green Strip

The green strips were sintered in a one-end closed muffle type furnace. The heating chamber, which was heated by silicon carbides rods, consisted of an Inconel tube, 750 mm long and of 100 mm internal diameter and was closed from one end. The constant temperature hot zone of size 15 mm was at the closed end of the furnace. The open end of the furnace had 200 mm long cooling chamber where the sintered strips were cooled under protective atmosphere. Gases were introduced at the closed end of the chamber through a 5 mm diameter Inconel tube passing through the open end of the chamber.

The dried green strips were sintered at 1273K for 3600s in dry hydrogen gas atmosphere. After sintering, the strips were slowly transferred into the cooling zone of the furnace where they were cooled in hydrogen atmosphere.

3.5 Hot Densification Rolling of the Sintered Strips

The sintered strips were porous and contained about 40% porosity. Therefore in order to make a fully dense strip, these were hot rolled. A small hole was drilled near one end of the sintered strip through which a thin nichrome wire was fastened which was required for pulling the hot strip through the rotating rolls during hot rolling operation. The sintered strips fastened with a nichrome wire were slowly introduced one at a time into the hot zone of a specially designed reheating furnace interlinked with a two high rotating mill. Preheating for each strip was done at 1273K for 1800s in dry hydrogen atmosphere. Hot rolling was done on a single stand, non-reversing type two-high rolling mill, having 135 mm diameter rolls, rotating at a fixed speed of 55 r.p.m. The preheating furnace was interlinked with the rolling mill in such a manner that the strips remained in the protective atmosphere up to the roll nip. Thickness reduction was achieved by pulling the strip by the wire fastened to it and forcing the hot strip through the rotating rolls set at a pre-determined roll gap. Soon after rolling the strip were cooled in a bed of fine graphite powder to prevent oxidation of the strip. After each pass, the strip was subjected to grinding in order to remove any edge crack formed during rolling, in order to avoid the growth of the cracks in the subsequent pass. The sintered strips were hot rolled to 42%, 52%, 61%, 72%, 82%, 88%, 92% and 96% thickness reduction. Up to 50% thickness reduction, it was possible to hot roll in a single pass. Beyond it, hot rolling was done in more than one pass.

Some sintered strips prepared from 95Cu-5W and 90Cu-10W powders were hot rolled to only 82% thickness reduction, for studying the effect of amount of tungsten on the hot rolled copper-tungsten composite strips.

3.6 Annealing after Hot Rolling

During hot rolling, the hot rolls were not preheated; therefore when hot sintered strips came in contact with the cold rolls, there was a chilling effect, in particular, on the surfaces of the strip. This would bring down the temperature of the surface layers leading to warm working condition. Also, there could be some surface oxidation of the strip during and just after hot rolling, despite the fact that the strip was exposed to atmosphere during rolling for a very short period of time, and it was cooled in a graphite bed after rolling. The surface oxides were reduced by annealing the strip in hydrogen atmosphere. The annealing operation also removed any work hardening brought about by chilling caused by cold rolls. Therefore, the densified strips after hot rolling were annealed at 1273K in dry hydrogen atmosphere for 900s in the horizontal tube Inconel furnace and cooled in the cooling zone of the furnace under the protective atmosphere. Thus, all the mechanical testing of the hot rolled copper-tungsten strips were done after annealing treatment.

3.7 Characterization Methods

High energy milled copper-tungsten powder was subjected to X-ray diffraction studies. The sintered and hot rolled annealed strips were tested for various mechanical and physical properties.

3.7.1 X-ray diffraction Analysis of Mechanical Milled Copper-Tungsten Powder

X-ray diffraction pattern for the high-energy milled copper-tungsten powder were obtained from the x-ray diffractometer model RICH SI EFERT ISO DEBYEF LEX 2002, Germany. Copper-k$\propto$ radiation was used for the x-ray diffractions studies.

3.7.2 Optical & Scanning Electron Microscopy

Microstructures of hot rolled strips rolled to different rolling reductions were observed under optical microscope. For observing the microstructure and to prevent the pores from being filled by ductile copper during polishing operations, the porous hot rolled strips were first impregnated in vacuum with low viscosity cold settling resin. Araldite A.Y.103 and a hardener H.Y.951, manufactured by Ciba Speciality Chemicals (Inds) Ltd. were used for this purpose. The ratio of araldite to hardener was 100:9. Sample preparation for the micro structural studies consisted of standard emery paper polishing followed by fine cloth polishing with alumina abrasive particles in suspension with water. Some polished specimens of hot rolled copper-tungsten strips were also observed under scanning electron microscope.

3.7.3 Particle Size Distribution Analysis

Size distribution of the second phase tungsten particles was carried out in image analyzer. Before studying the particle size distribution, the samples were polished by emery paper and then by wheel polishing.

3.7.4 Microhardness Measurement

Microhardness of the copper-tungsten composite strips was measured in MHP 160 Microhardness Tester. A diamond pyramid indenter was used. Load of 160 gm was used for the indentation purpose. It was applied for a short period of time i.e. 3s. Indentation was done at the Cu/W interface so that it was partly on the copper matrix and partly on the tungsten particle. From the average value of the measured diagonal length, microhardness was determined. Well-polished samples of copper-tungsten strips were used for determination of the microhardness. It was determined from the following formula:

$$H_v = 1.854\ P/\ L^2 \qquad (3.1)$$

where, P is load in kg and L is the average length of the diagonals.

3.7.5 Tension Testing

Ultimate tensile strength, 0.2% proof strength and percentage elongation were measured by uniaxial tension testing on an INSTRON-1195 machine The testing was done at room temperature and at a crosshead speed of 0.5-mm/min and chart speed of 20mm/min. the specimen used for tension testing was not standard type, due to shortage of material. Therefore a non-standard specimen was used for tension testing. However, the geometry of the specimen was kept same as that of the standard specimen. The dimensions of the tension test specimen are shown in Figure 3.3. For each tension test three specimens were subjected to testing and the average value of the tensile strength, percentage elongation and proof strength were taken.

3.7.6 Density Measurement

Green density, sintered density and density of copper-tungsten strip hot rolled up to 82% were determined by measuring the dimensions and the weight. Density of copper-tungsten strip hot rolled above 82% was measured by displacement method using the Archimedes principle. The density of each sample was measured three times and then averaged. The theoretical density was determined on the basis of rule of mixture, as follows:

$$\text{Theoretical density} = \rho_{Cu}\, w_{Cu} + \rho_{w}\, w_{w} \qquad (3.2)$$

where, ρ and w are actual density and weight fraction respectively.

The ability to which copper-tungsten composite can be densified by sintering is expressed by densification parameter. It is expressed by following relationship.

$$\text{Densification parameter} = (sd\text{-}gd) / (td\text{-}gd) \qquad (3.3)$$

where, gd, sd and td are green density, sintered density and theoretical density respectively.

The efficiency of densification by hot rolling is calculated by the following relationship:

$$E = (\rho_{HR}-\rho_o) / (\rho-\rho_o) \quad (3.4)$$

where, ρ_{HR} is density of hot rolled Cu-W composite strip, ρ_o is the density Cu-W composite strip before rolling i.e. sintered density and ρ is the theoretical density.

3.7.7 Electrical Conductivity Measurement

Electrical conductivity was measured by conductivity meter Type 979 (Techno four). It is a lightweight portable instrument designed to measure electrical conductivity of non-ferrous metals in %IACS (International Annealed Copper Standard). During calibration, both hi-set and low-set knobs were kept at position 5.0. The probe was then placed firmly within the encircled area on the high value sample. After adjusting hi-set knob, the probe was placed within the encircled area on the low value sample. This was repeated until readings as per standard sample plate was obtained. Finally, after adjustment, the readings of the copper-tungsten strips were taken at various places. Before taking readings, the samples were slightly polished for making full contact of probe with the sample.

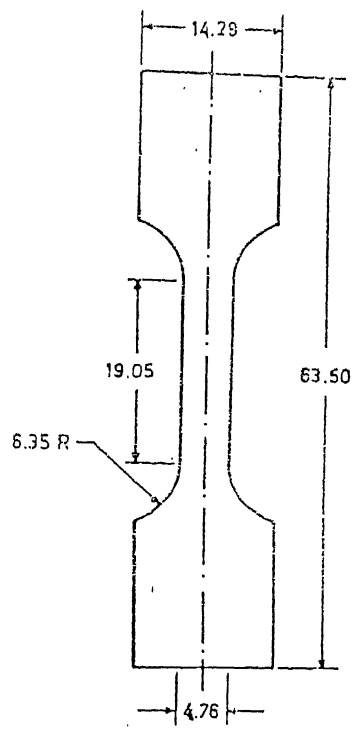

Figure 3.3: Tensile test specimen (units in mm) [52]

CHAPTER 4

RESULTS & DISCUSSION

4.1 Characterization of High Energy Milled Cu-W Powder

4.1.1 X-ray Diffraction Studies

X-ray diffraction pattern (% Intensity vs. angle in degrees) of high energy milled 80Cu-20W composite powders milled for 16 hours is illustrated in Figure 4.1. There are peaks of pure copper, pure tungsten, tungsten oxide and mixed copper-tungsten oxide. It confirms that no other metastable copper-tungsten phases are formed after high-energy milling. Since copper and tungsten are completely insoluble, 16 hours milling is insufficient for obtaining metastable phases.

4.2 Properties of "Green" Cu-W Composite Strips

The green densities of the copper-tungsten composite strips containing 5, 10, 20 and 30wt% of tungsten are shown in Table 4.1. The Table also shows the theoretical density of each composition on the basis of rule of mixture as given in equation 3.2.

Table 4.1 Green density of copper-tungsten composite strips

Composition	Theoretical Density gm/cc	Density of green strip, gm/cc	% Theoretical Density of the green strip
95Cu-5W	9.446	2.79	29.5
90Cu-10W	9.962	2.80	28.2
80Cu-20W	10.996	2.82	25.7
70Cu-30W	12.026	3.02	25.1

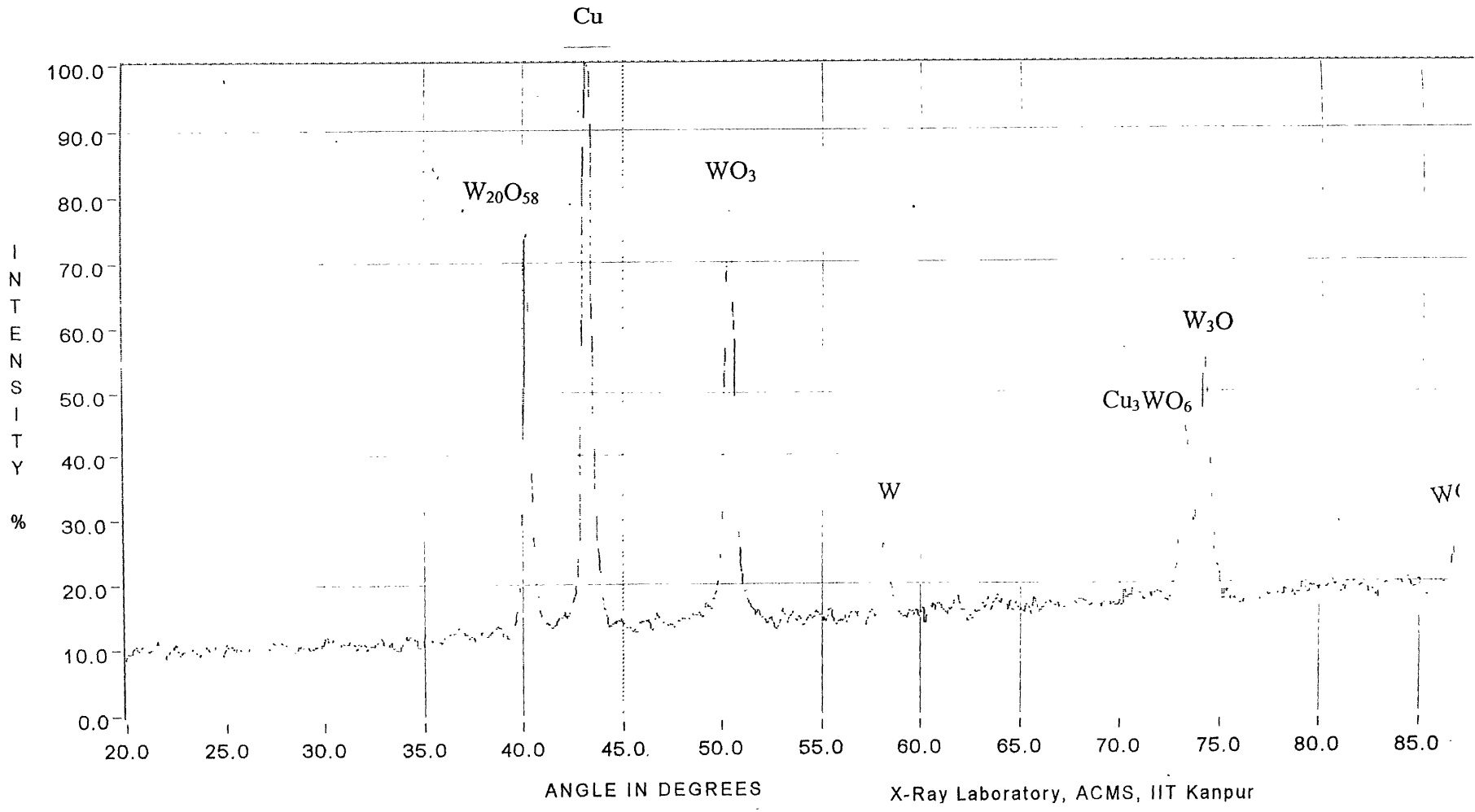

Figure 4.1: X-ray diffraction pattern of 80Cu-20W composite powders milled for 16 hours

Tungsten has higher density (19.25 gm/cc) as compared to copper (8.93 gm/cc), so as the amount of tungsten increases its green density also increases. The variation of the percentage theoretical density with the amount of the tungsten content is shown in Figure 4.2. It decreases with increasing amount of the tungsten content. As obvious, the amount of porosity content in the copper-tungsten strip increases with increase in tungsten content.

4.3 Properties of Sintered Cu-W Composite Strips

The densities of the copper-tungsten composite strips containing 5, 10, 20 and 30wt% of tungsten after sintering at 1273K are shown in Table 4.2.

Table 4.2 Sintered density of Cu-W strips of various compositions

Composition	Apparent density after sintering, gm/cc	% Theoretical Density of the sintered strip
95Cu-5W	3.96	41.9
90Cu-10W	3.50	35.0
80Cu-20W	3.55	32.3
70Cu-30W	3.19	26.6

Figure 4.3 gives the variation of percentage theoretical density with tungsten content of sintered samples. It decreases with increasing amount of the tungsten. Further it can be seen that the density of 80Cu-20W strip increases from 25.7% theoretical density at green strip stage to 32.3% theoretical density after sintering. This shows that only a minimal amount of sintering has taken place. It should be noted that the temperature of 1273K is quite adequate for the sintering of copper particles, but is not for tungsten particles. Tungsten hinders the solid state sintering of the copper-tungsten strip so with increasing tungsten content low percentage of theoretical density is obtained. During sintering of copper-tungsten composites, tungsten particles on the surface of the

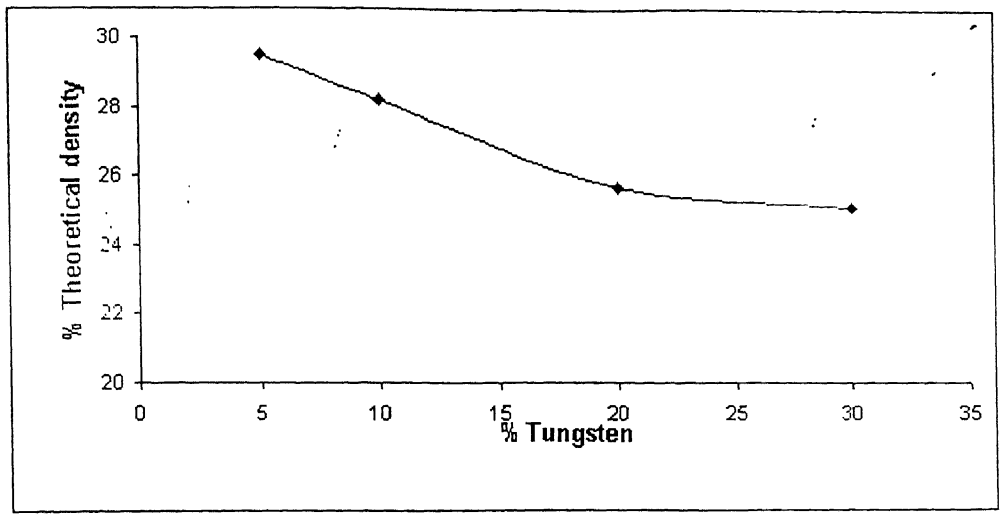

Figure 4.2: Variation of % theoretical density with weight % tungsten of green Cu-W composite strips

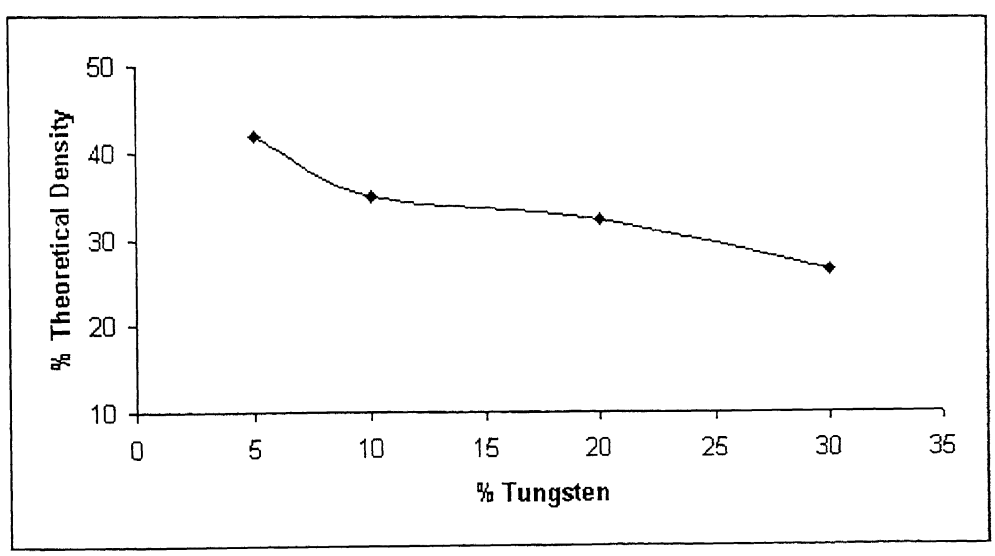

Figure 4.3: Variation of % theoretical density with weight % tungsten of sintered Cu-W composite strips

composite powders hinder copper neck formation and hence shrinkage. Since there is no solid solubility between copper and tungsten particles, bonding between copper and tungsten particles is poor during solid state sintering.

The sintered 70Cu-30W strips did not have adequate strength, and presented problems in handling leading to breakage of the strip.

Densification parameter for copper-tungsten composites containing 5, 10, 20 and 30wt% of tungsten are given in Table 4.3. Figure 4.4 gives the variation of the densification parameter with tungsten content. It was calculated using equation 3.3. With increasing tungsten content densification parameter decreases which shows that efficiency of densification is poor in copper-tungsten composite containing higher amount of tungsten. The reason for poor densification has been already explained

Table 4.3 Densification parameter for Cu-W strips of various compositions

Composition	Densification parameter
95Cu-5W	0.18
90Cu-10W	0.10
80Cu-20W	0.09
70Cu-30W	0.02

The optical micrographs of the sintered copper-tungsten composite strip are shown in Figure 4.5a, 4.5b, 4.5c and 4.5d. It can be seen that from Figure 4.5a that there is considerable amount of porosity in the strip, which is corroborated by the density measurement values. Both irregular and elongated copper particles are present in the sintered strip as shown in Figure 4.5b. Further, the tungsten particles are embedded within the copper particles as shown in Figure 4.5c, and are also present on the surface (Fig.4.5c & 4.5d). As explained earlier, the tungsten particles are inhibiting the process of sintering of copper at 1273K.

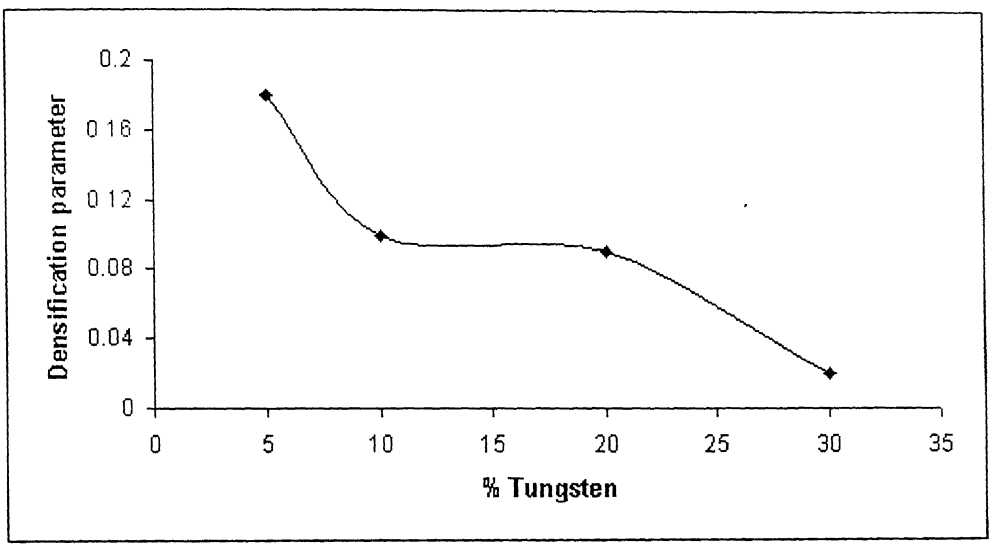

Figure 4.4: Densification parameter as function of tungsten content

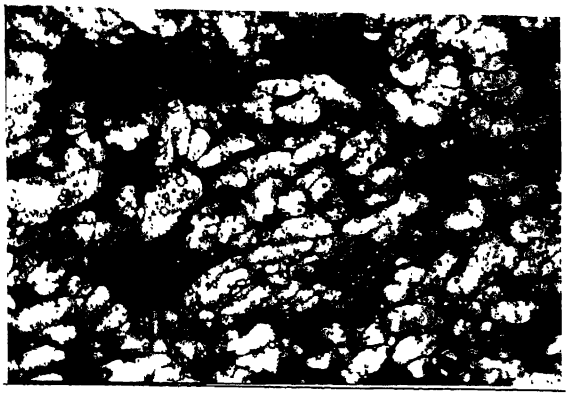

(a) X200

(b) X500

Figure 4.5: Optical micrographs of sintered 70Cu-30W composite strip (unetched)

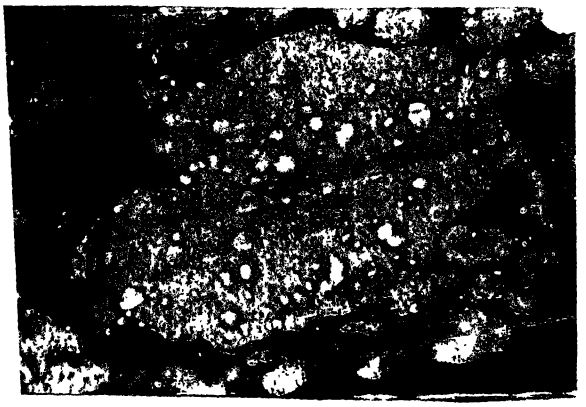

(c) X500

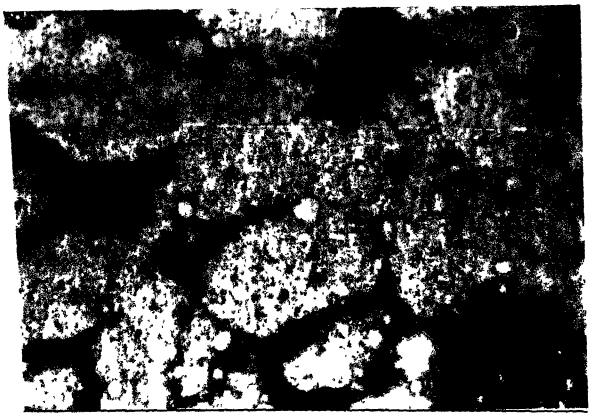

(d) X1000

4.4 Hot Densification Rolling of Sintered 80Cu-20W Composite Strips

This section describes the effect of percentage thickness reduction by hot rolling on the structure and properties of 80Cu-20W composite strips.

4.4.1 Effect of Hot Densification Rolling on the Density of 80Cu-20W Composite Strips

The apparent density of the 80Cu-20W strips obtained after hot rolling the sintered strip at 1273K to various percentage thickness reductions are shown in Table 4.4.

Table 4.4 Density of hot rolled Cu-W composite strips

% Thickness reduction by hot rolling	Apparent density or actual density, gm/cc	% Theoretical density
42	5.37	48.8
52	6.34	57.7
61	7.11	64.6
72	8.56	77.9
82	9.82	89.3
88	9.70	88.2
92	9.68	88.0
96	9.61	87.4

It can be seen that a maximum density of 9.82 gm/cc was obtained at a hot rolling thickness reduction of about 82%. This density value corresponds to about 90% of the theoretical density. The Figure 4.6 illustrates the variation of density with the amount of hot rolling thickness reduction given to the 80Cu-20W sintered strips at 1273K. It can be seen that the percentage theoretical density increases linearly with increasing amount of hot reduction up to 82% of hot rolling. Beyond 82% hot reduction, there is slight decrease in density.

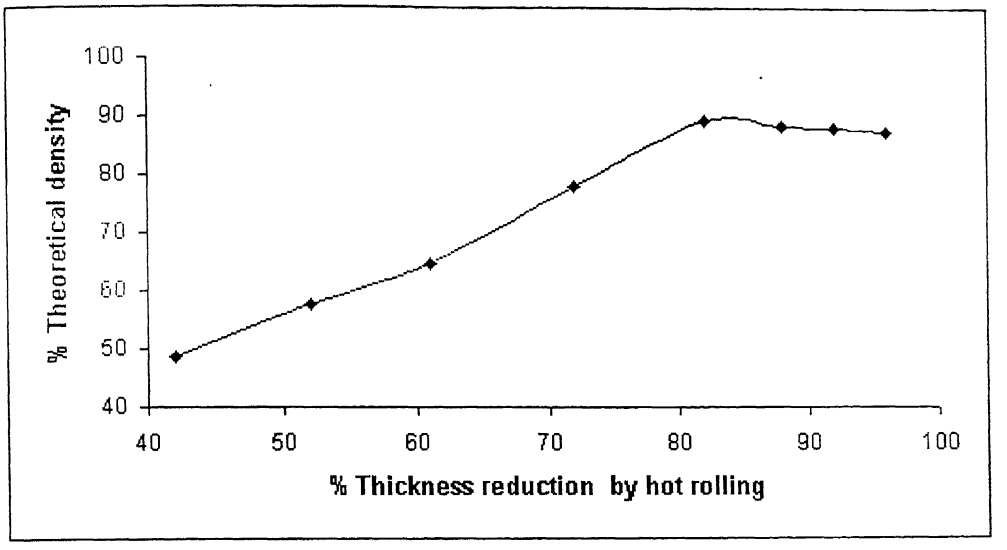

Figure 4.6: Variation of % theoretical density with the amount of hot rolling thickness reduction of 80Cu-20W composite strips

Figure 4.7 and Table 4.5 show the efficiency of hot densification rolling. The efficiency was calculated using equation 3.4, and is shown as continuous line. The dotted line shows the relationship between efficiency of hot densification rolling and percentage thickness reduction by hot rolling assuming that all the deformation was used in closing the pores of the composite copper-tungsten strip without any increase in length. It is assumed that the deformation takes place in plane strain condition.

Table 4.5 Efficiency of hot densification rolling of 80Cu-20W composite strips

% Thickness reduction by hot rolling	Theoretical efficiency, %	Actual efficiency, %
0	0	0
42	34.5	24.4
52	51.7	37.5
61	74.5	47.8
72	100	67.3
82	100	84.2
88	100	82.6
92	100	82.3
96	100	81.4

4.4.2 Effect of Hot Densification Rolling on the Mechanical Properties of 80Cu-20W Composite Strips

The room temperature mechanical properties of the hot rolled and annealed 80Cu-20W composite strips at various hot rolling thickness reductions are shown in Table 4.6. The annealing was done to remove any hardening induced in the strip due to temperature drop brought about by the contact of hot composite strip with cold rolls of the rolling mill during hot rolling.

Table 4.6 Mechanical properties of hot rolled Cu-W composite strips

% Thickness reduction by hot rolling	Ultimate tensile strength, M Pa	0.2% proof strength	% Elongation	Microhardness, kg/mm^2
42	20	19	1	107.1
52	38	37	1	110.8
61	62	42	2	112.5
72	141	74	4	117.6
82	281	104	21	126.8
88	272	115	20	127.3
92	227	121	19	127.0
96	220	126	14	126.9

Figure 4.8 shows the variation of ultimate tensile strength with the amount of percentage hot rolling thickness reduction. The ultimate tensile strength of the hot rolled and annealed strip increases slowly between 40% and 60% thickness reduction by hot rolling. Beyond 60% thickness reduction, the ultimate tensile strength of the hot rolled and annealed strip increases rapidly and reaches a maximum value at about 82% hot rolling thickness reduction. It can also be noted that the ultimate tensile strength starts decreasing as the strip is further hot rolled beyond 82% hot rolling thickness reduction.

Figure 4.9 shows the effect of percentage hot rolling thickness reduction on the 0.2% proof stress of the 80Cu-20W composite strips in hot rolled and annealed condition. It can be seen that the 0.2% proof stress is increasing continuously with percentage hot rolling thickness reduction.

Figure 4.10 shows the effect of percentage hot rolling thickness reduction on the percentage elongation of the 80Cu-20W composite strips in hot rolled and annealed condition. It is apparent that there is not much change in percentage elongation of the strip up to about 65% thickness reduction by hot rolling. However, beyond this value of

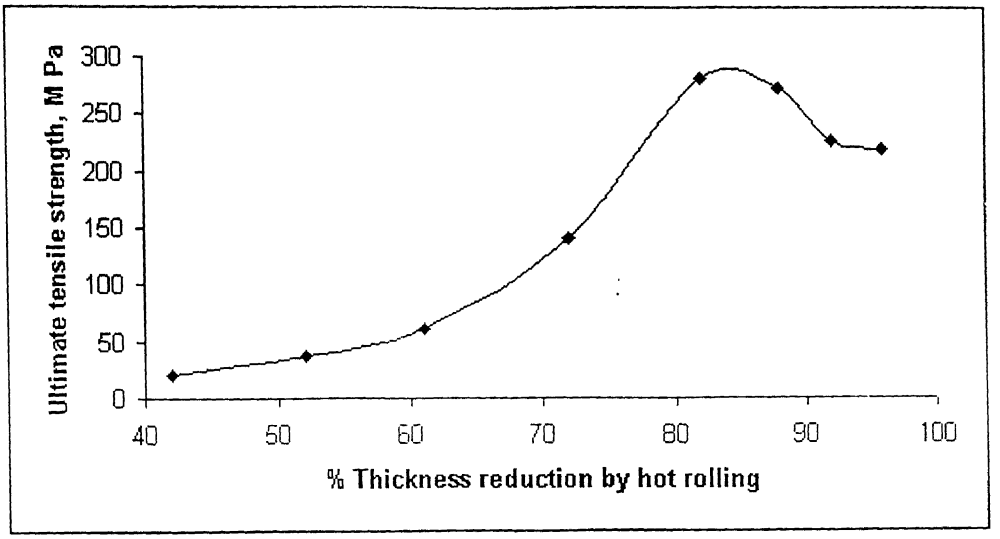

Figure 4.8: Variation of ultimate tensile strength with the amount of % hot rolling thickness reduction of 80Cu-20W composite strips

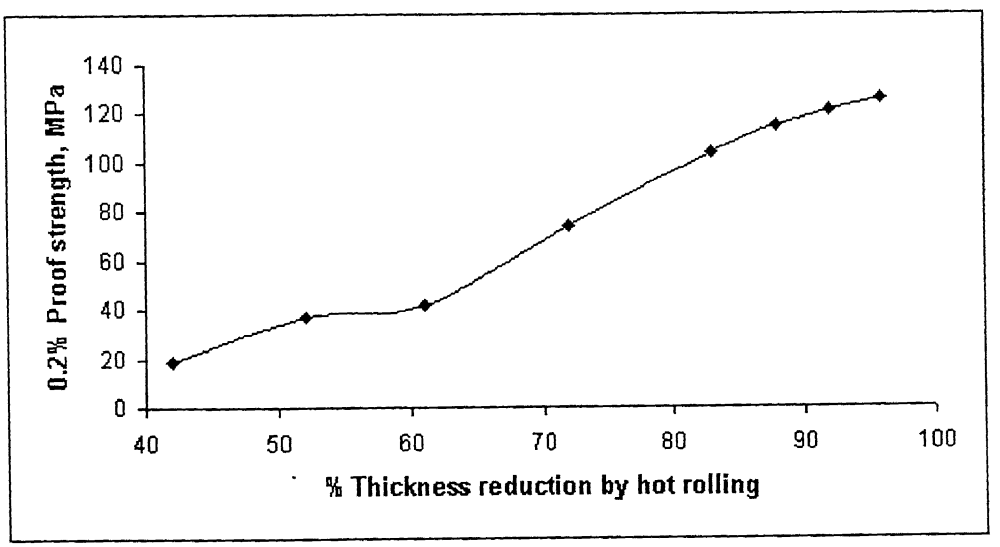

Figure 4.9: Variation of 0.2% proof strength with the amount of % hot rolling thickness reduction of 80Cu-20W composite strips

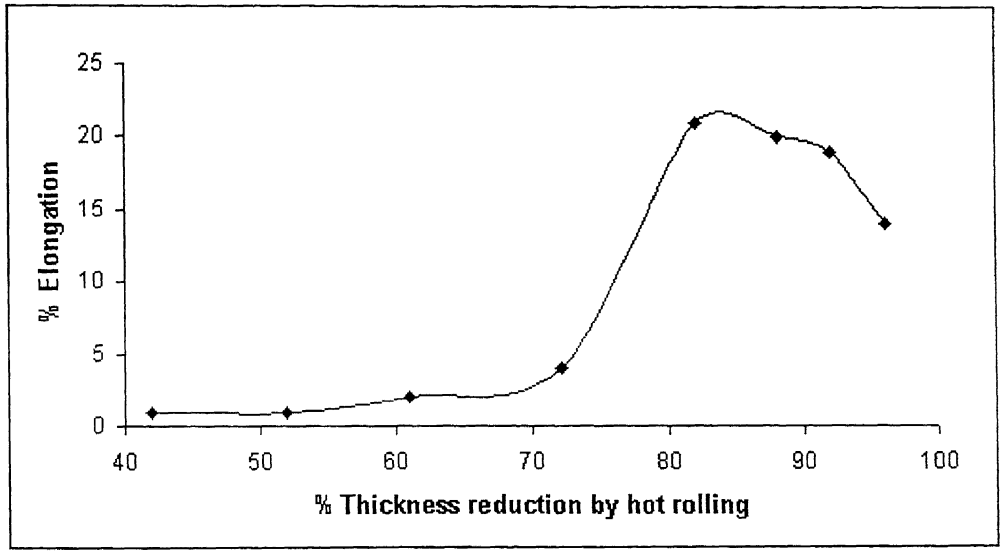

Figure 4.10: Variation of % elongation with the amount of % hot rolling thickness reduction of 80Cu-20W composite strips

hot rolling reduction the percentage elongation increases very rapidly as hot rolling continues, and reaches a maximum value of about 21% at about 82% hot rolling thickness reduction. As the hot rolling is continued further beyond 82% thickness reduction, the percentage elongation decreases. It is also interesting to note that both the ultimate tensile strength and percentage elongation of the strip decrease beyond 82% hot rolling thickness reduction. However, the rate of decrease of the percentage elongation is faster than that of decrease of ultimate tensile strength.

Figure 4.11 shows the effect of percentage hot rolling thickness reduction on the microhardness of the 80Cu-20W composite strips in hot rolled and annealed condition. It is apparent that the microhardness of the strip increases up to 82% thickness reduction, and then remains more or less constant. Increase in hardness up to 82% thickness reduction is due to two factors. Firstly, the porosity is continuously decreasing as the percentage hot rolling thickness reduction increases. Secondly, at the hot rolling temperature of 1273K copper is getting hot worked, but tungsten is getting cold worked. Therefore, the hardness of tungsten particles is increasing with percentage thickness reduction by hot rolling.

4.4.3 Structural changes in the 80Cu-20W Composite Strips during Hot Densification Rolling

The optical micrographs of the hot rolled 80Cu-20W composite strips rolled to 42%, 52%, 61%, 72%, 82% and 96% thickness reductions are shown respectively in Figure 4.12, 4.13, 4.14, 4.15, 4.16 and 4.17 at its cross-section parallel to rolling direction. As it can be seen that the porosity in the strip is continuously decreasing as the percentage thickness reduction by hot rolling is increasing. At low value of hot rolling reduction, say 42%, the contact area between the particles are small. The microstructure consists of irregular and as well elongated particles. As the hot rolling thickness reduction increases from 42%, the contact area between the particles also increases. At about 61% thickness reduction considerable elongation of copper particles starts taking place (Fig.4.14). At about 72% thickness reduction, the individual particles are not identifiable

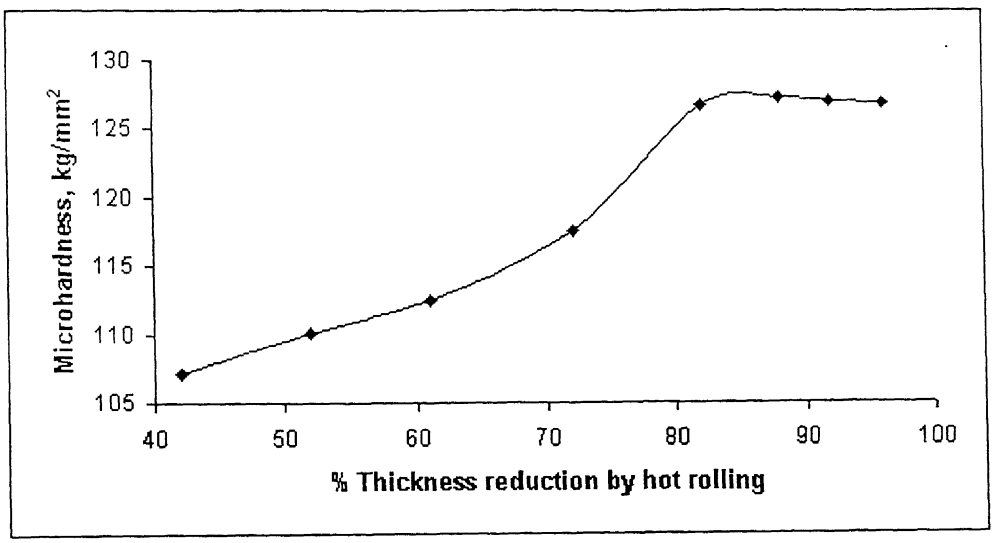

Figure 4.11: Variation of microhardness with the amount of % hot rolling thickness reduction of 80Cu-20W composite strips

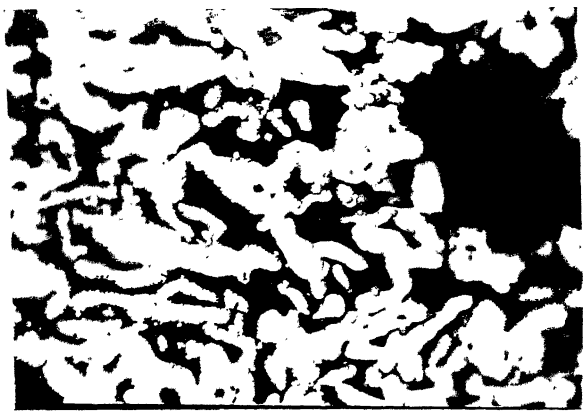

(a) X500

(b) X500

(c) X500

Figure 4.12: Optical micrographs of 80Cu-20W composite strip hot rolled to 42% of thickness reduction (unetched)

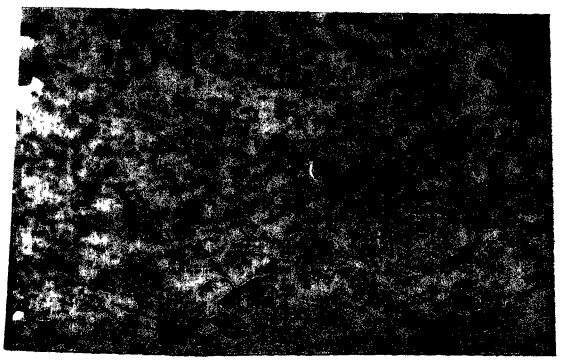

(a) X200

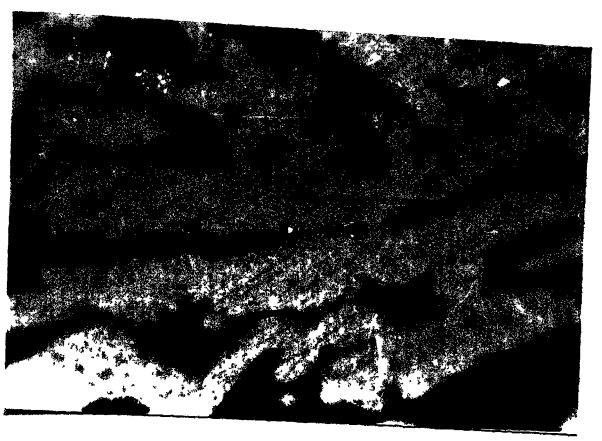

(b) X1000

Figure 4.13: Optical micrographs of 80Cu-20W composite strip hot rolled to 52% of thickness reduction (unetched)

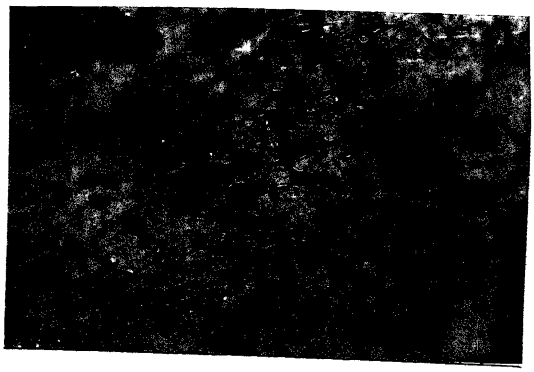

(c) X500

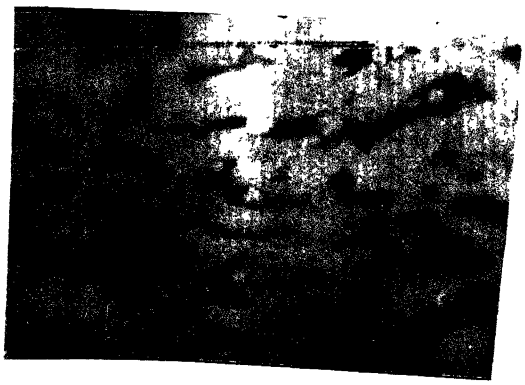

(d) X1000

(a) X1000

(b) X1000

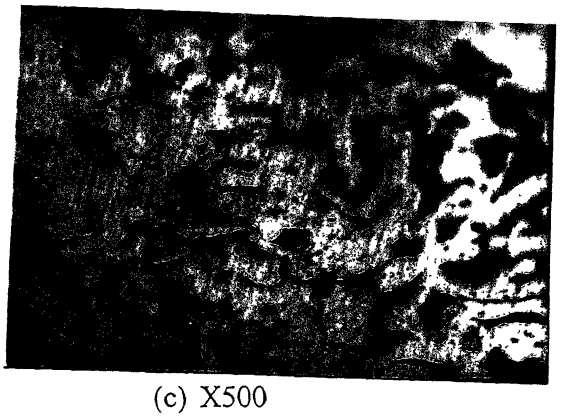

(c) X500

Figure 4.14: Optical micrographs of 80Cu-20W composite strip hot rolled to 61% of thickness reduction (unetched)

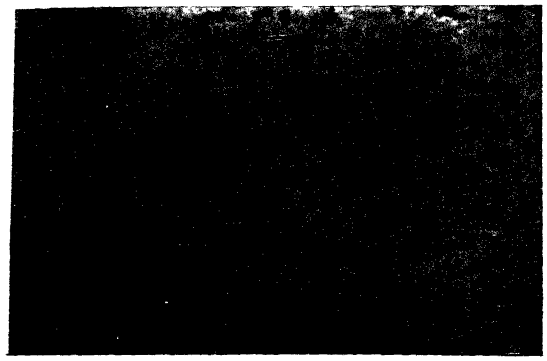

(a) X200

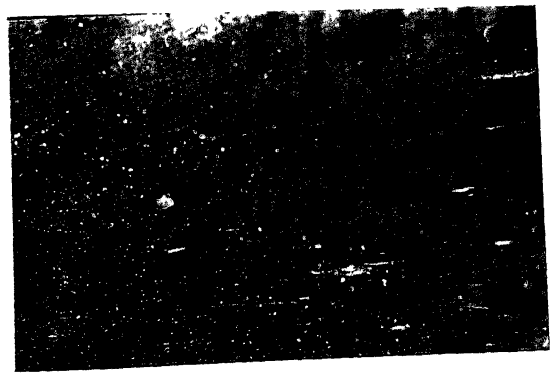

(b) X500

(c) X1000

Figure 4.15: Optical micrographs of 80Cu-20W composite strip hot rolled to 72% of thickness reduction (unetched)

(a) X500

(b) X1000

(c) X200

Figure 4.16: Optical micrographs of 80Cu-20W composite strip hot rolled to 82% of thickness reduction (unetched)

(a) X1000

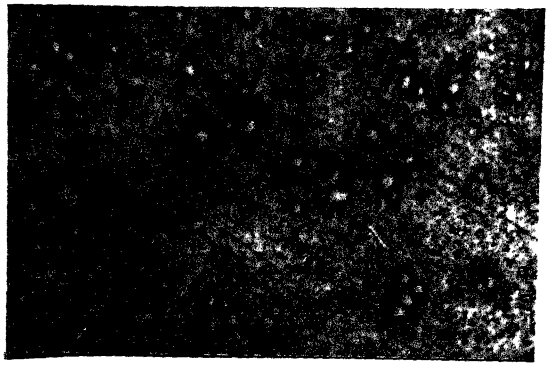

(b) X500

Figure 4.17: Optical micrographs of 80Cu-20W composite strip hot rolled to 96% of thickness reduction (unetched)

as they have joined together completely with the neighbouring particles. Porosity is evenly distributed. At 82% thickness reduction, the nature of the structure of the strip is similar to that of the strip hot rolled to 72% thickness reduction. However, the amount of porosity is lower in the former case.

An interesting feature is observed in the microstructure of the 80Cu-20W strip hot rolled to 96% thickness reduction. Micro-cracks appear around the tungsten particles as shown in Figure 4.17a. Also some porosity can be seen.

Figure 4.18 shows the scanning electron micrographs of polished 80Cu-20W strips subjected to 91% thickness reduction by hot rolling at its cross-section parallel to rolling. It can be seen that there are uniformly distributed small size tungsten particles and also some clusters of tungsten particles (Fig.4.18a). The cluster of tungsten particles are somewhat aligned in the direction of hot rolling. The figure also gives a general view of the cracks formed within the strips, which is described later. The fracture of bigger tungsten particles can also be seen from Figure 4.18b, 4.18c and 4.18d. Further, crack formation at the Cu/W interface is also taking place. This occurs first on the interface between copper and bigger size tungsten particles (8-10μm), as shown in Figure 4.18c. At this amount of hot rolling, there is no crack formation at the interface between copper and small size tungsten particles (1-2μm), as shown in Figure 4.18e.

Figure 4.19 illustrates the size distribution of tungsten particles in 80Cu-20W composite strip hot rolled to 82% thickness reduction. The mean size of tungsten particles is 2.89 μm. From this curve it is clear that there are some tungsten particles whose size is between 10 μm to 30 μm.

4.4.4 Effect of Hot Densification Rolling on the Electrical Conductivity of 80Cu-20W Composite Strips

Table 4.7 and Figure 4.20 show the effect of hot rolling thickness reduction on the electrical conductivity of copper-tungsten composite strips. Maximum value of electrical

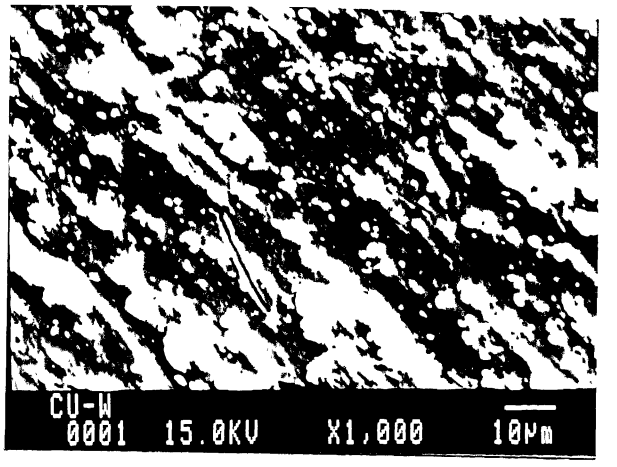

(a)

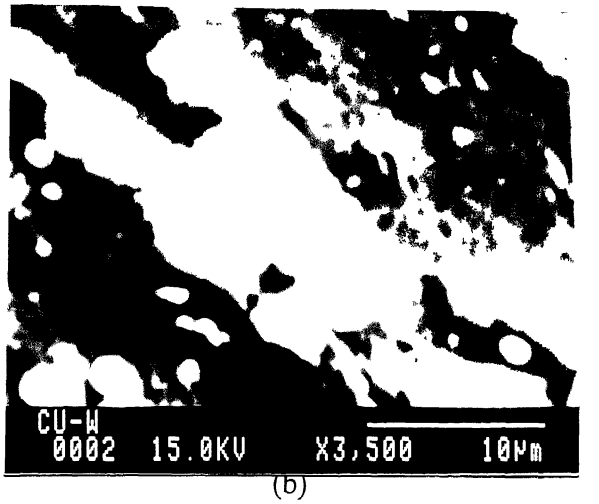

(b)

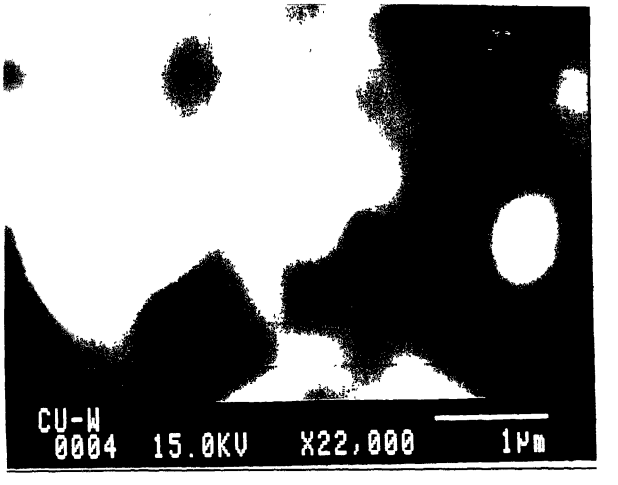

(c)

Figure 4.18: SEM micrographs of 80Cu-20W composite strip hot rolled to 91% of thickness reduction (unetched)

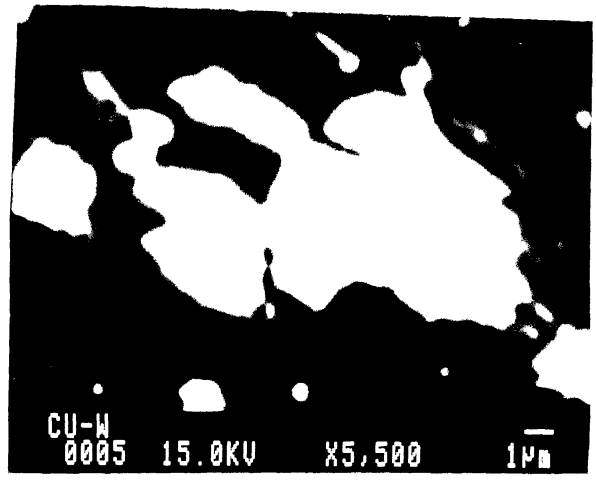

(d)

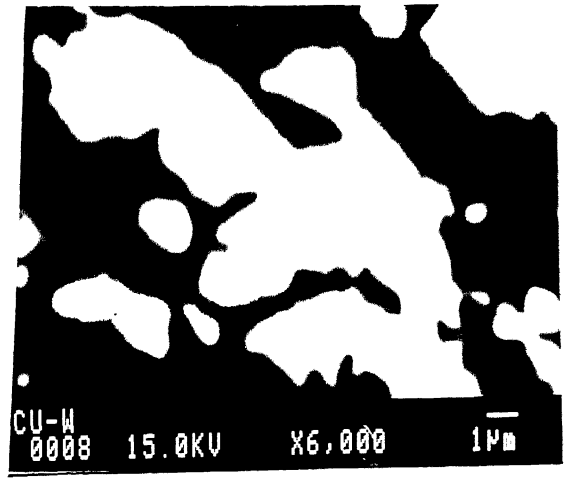

(e)

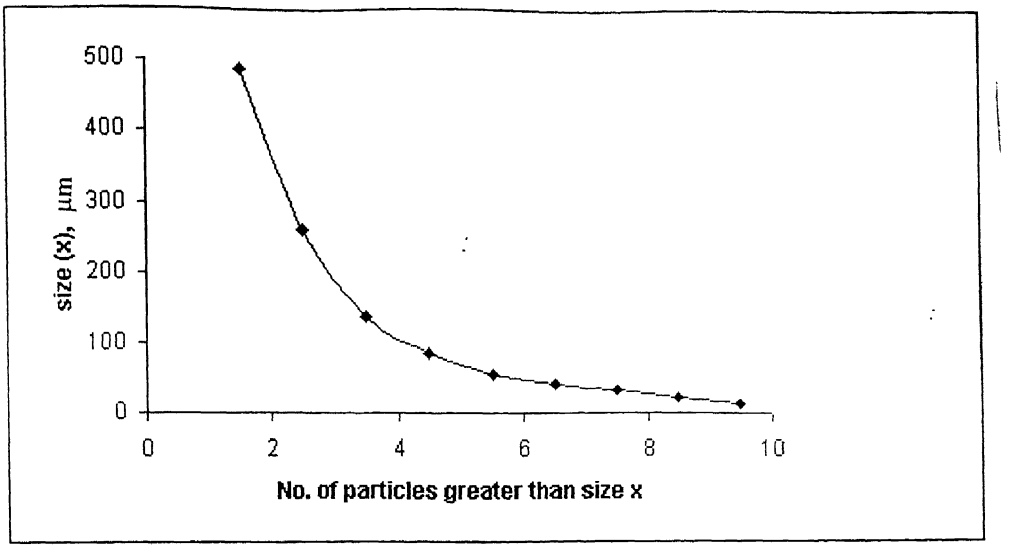

Figure 4.19: Size distribution of tungsten particles in 80Cu-20W composite strip hot rolled to 82% of thickness reduction

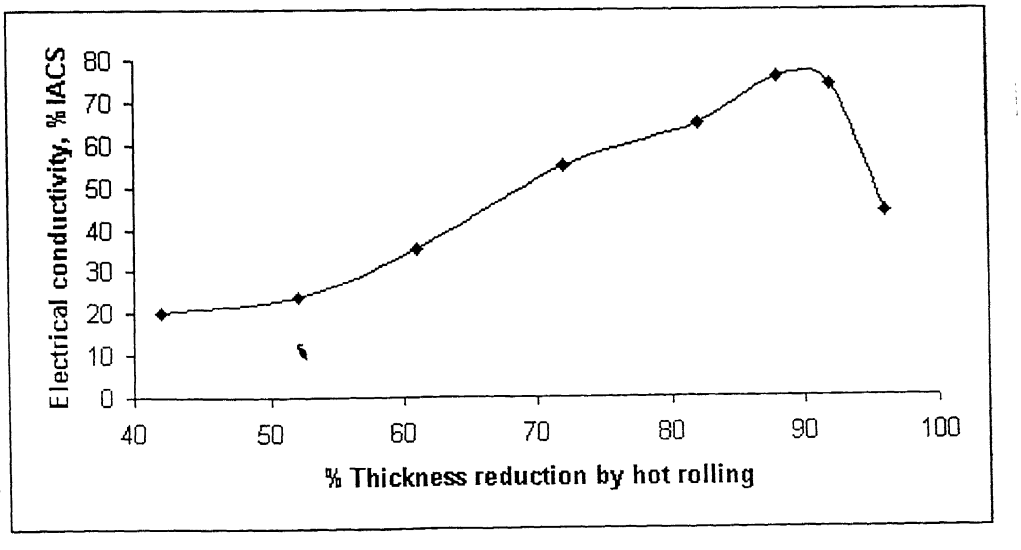

Figure 4.20: Variation of electrical conductivity with the amount of % hot rolling thickness reduction of 80Cu-20W composite strips

conductivity is 76% IACS which is obtained at 88% of hot reduction. Electrical conductivity increases with the hot reduction but at 96% of hot reduction very low value of electrical conductivity is obtained.

Table 4.7 Electrical conductivity of hot rolled Cu-W composite strips

% Thickness reduction by hot rolling	Electrical conductivity, %IACS
42	20
52	24
61	35
72	55
82	65
88	76
92	70
96	44

The effect of hot rolling on the electrical conductivity of copper-tungsten composite can be explained in the light of the microstructural changes occurring during hot rolling as explained earlier. The initial increase in the electrical conductivity is due to the decrease in the amount of porosity. Presence of porosity decreases the overall area available for the flow of the current. As the amount of the porosity decreases, area available for the flow of the current increases which results in the increase in the electrical conductivity. As shown earlier, maximum density was achieved at about 82% thickness reduction by hot rolling. Beyond this value of thickness deformation, crack formation at the Cu/W interface starts taking place together with the fracture of tungsten particles. This leads to decrease in electrical conductivity beyond about 88% thickness reduction by hot rolling. The electrical conductivity of pure copper and pure tungsten at room temperature are 100 %IACS and 31 %IACS respectively [53]. So the electrical conductivity of 80Cu-20W composite strip obtained from rule of mixture is 86.2 %IACS.

4.5 Densification & Deformation behaviour of Cu-W Composite Strip during Hot Rolling: A General Discussion

During hot densification rolling of 80Cu-20W composite strip, both densification and deformation of the strip are taking place. Such behaviour of the porous strip during hot densification rolling can be understood in terms of the movement of copper and tungsten particles. As explained earlier no significant amount of sintering has taken place in the sintered copper-tungsten strip after sintering and therefore the area of cross section of neck region between various particles would be small in the starting strip for hot rolling.

The densification and deformation behaviour of porous 80Cu-20W composite strip can be divided into three stages

(1) Stage I: This stage can be identified up to about 60% thickness reduction by hot rolling.

(2) Stage II: This stage can be identified between ~60% and ~82% thickness reduction by hot rolling.

(3) Stage III: This stage can be identified beyond ~82% thickness reduction and up to ~96% thickness reduction in the present study.

When sintered 80Cu-20W porous strip is hot rolled, stresses are applied on each particle. In the initial stage of hot rolling, the overall stresses acting on the strip are too small to cause any significant plastic deformation of the particles. Owing to the smaller area of cross-section of the neck regions between various particles, stress concentration was higher at such points than in the bulk of the particles. Therefore, during the initial stage of hot rolling i.e. stage I, particles would slide at the neck region and some particle rotation would also be observed. A typical particle rotation can be seen in Figure 4.12b and 4.12c. The particles would move into the adjoining pore area, depending upon the restraints present in the vicinity of the particle. For example, as shown in Figure 4.12c, some elongated particles, which were earlier aligned longitudinally, have rotated to about 90^0.

Further there would also be frictional resistance at the interface of copper and tungsten particles [54]. As a result, the flow of copper on the surface of tungsten would be affected. This aspect of flow can be visualised in Figure 4.13d in which it can be seen that some copper in the neighbourhood of tungsten particle is flowing in the longitudinal direction on a micro scale instead of flowing in the thickness direction due to friction offered by the tungsten particles.

In this stage, the overall affect of hot rolling is the rearrangement and restacking of the particles. The contact between particles continuously increases, but the overall contact area is not large. This results in the continuous increase in the ultimate tensile strength of the strip as the percentage thickness reduction by hot rolling increases, as shown in Figure 4.8. However, the overall increase is not very significant in absolute terms. The increase in percentage elongation is insignificant, as it is greatly dependent on the total amount of porosity, which is still large.

The onset of stage II is characterised by the rapid increase in the interparticle contact area. Stage II is also accompanied with a substantial plastic deformation of particles (Figure 4.14a & 4.14b). As it can be seen from Table 4.4 and Figure 4.6, the density of 80Cu-20W composite strip after~ 61% thickness reduction is~ 65% of the theoretical density. At the end of stage I, it appears that particles have rearranged and restacked to a maximum possible packing density when no further densification without significant longitudinal flow is possible by hot rolling. It is interesting to note that in an earlier study on the hot rolling of porous copper strip it was found that longitudinal flow in copper particles become predominant when the density of strip has attained a value of ~70% of theoretical density [55]. However, it must be kept in mind that there would also be some overlapping of stage I and stage II during the hot rolling process. Another interesting feature of stage II is that the mechanical properties, viz UTS and % elongation increase very rapidly with percentage thickness reduction by hot rolling. This behaviour can be explained by the earlier stated observation of particle elongation, significant increase in interparticle contact area, and continuous decrease in porosity.

Further it can also be observed that the 80Cu-20W composite strip at the end of stage II (i.e. after ~82% thickness reduction) is not fully dense. However the mechanical properties of the 80Cu-20W composite strip after ~82% thickness reduction by hot rolling is rather interesting. The strip has UTS of 281MPa, 0.2% proof stress of 104 MPa and elongation 21%. The properties show that it is a useful material and can be used for making electrical contacts of various designs. It is interesting to compare the above mechanical properties with those of pure copper, as follows [56]

Ultimate tensile strength = 220 MPa
0.2% Proof stress = 70 MPa
% Elongation = 50

As it can be seen from Figure 4.10 & 4.11, the UTS and percentage elongation of the 80Cu-20W composite strip decrease beyond ~82% thickness reduction by hot rolling i.e. stage III. The percentage theoretical density of the strip is also decreasing with increase in percentage thickness reduction by hot rolling in this stage (Figure 4.6).

The hot rolling of 80Cu-20W composite strip is actually hot rolling of a two phase material in which one phase i.e. copper is soft and ductile, and the other phase, i.e. tungsten is hard and brittle. Copper and tungsten particles would behave differently during hot rolling of composite copper-tungsten strip. Due to very high recrystallization temperature of tungsten, it would actually be cold worked at 1273K, while copper would be subjected to hot working. The ratio of deformation of tungsten to copper matrix deformation can be termed as relative plasticity (ν), as follows:

$$\nu = \varepsilon_w / \varepsilon_{cu}$$

where, ε_w = true strain in tungsten

ε_{cu} = true strain in the matrix, i.e. copper

Further, the ratio between the flow stress of tungsten and the flow stress of copper at the temperature of hot rolling can be defined by the term β as follows:

$\beta = \sigma_w / \sigma_{cu}$

where, σ_w = flow stress of tungsten

σ_{cu} = flow stress of copper

An idea about the deformation behaviour of 80Cu-20W composite strip in stage III can be obtained from the deformation behaviour of steels containing hard inclusions. It has been shown that the bonding of the inclusion-matrix interface plays an important role in controlling the plasticity of the inclusions. The value of β at which ν tends to zero is ~2 for interfaces which are poorly bonded, but is in excess of 6 for all bonded interfaces [57]. With a well bonded interface strain can be effectively transformed to the inclusion, which is therefore constrained to deform even at higher values of its flow stress relative to that of the matrix i.e. β factor. On the other hand, with a poorly bonded interface to the inclusion and some relative sliding occurs at the matrix/inclusion interface so that the matrix deform around the inclusion, rather than the inclusion itself deforming. In addition, the degree of interface bonding is important in controlling the de-cohesion which can occur during deformation, and the formation of cavities at the ends of non-deformable inclusions. At higher inclusion strength, the effect of interface bonding is very important, as it largely controls whether hard inclusions will deform.

Copper and tungsten have very poor solid solubility in each other [58]. Thus, the bonding between copper and tungsten particles would be poor [59] in the 80Cu-20W composite strip. It is apparent that in the present case, the tungsten particles would not deform relative to copper matrix. In view of higher value of flow stress of tungsten particles, well-known conical voids at the end of tungsten particles would form (Fig.4.18a). Further, the stresses in the stage III are relatively higher and this would lead to the fracture of tungsten particles. This would be another source of microcrack formation. At higher hot rolling reductions, these cracks would form together leading to formation of bigger cracks.

In summary, hot rolling of 80Cu-20W composite strip beyond ~82% thickness reduction brings about de-cohesion of tungsten particles from the copper matrix together with the fracturing of tungsten particles. This leads to the deterioration of mechanical properties such as UTS and % elongation, and also the density as the hot rolling continues beyond ~82% thickness reduction.

4.6 Effect of Tungsten Content on the density and Mechanical Properties of Cu-W Composite Strips

Table 4.8 gives the actual density of the copper-tungsten composite strips containing 5, 10 and 20 wt% of tungsten, which were subjected to 82% of thickness reduction by hot rolling.

Table 4.8 Density of Cu-W composite strips hot rolled to 82% thickness reduction

Composition	Apparent density, gm/cc	% Theoretical density
95Cu-5W	9.04	95.7
90Cu-10W	9.30	93.3
80Cu-20W	9.82	89.3

Copper-tungsten composite containing 5% of tungsten has less porosity i.e. 4% as compared to composite containing 20% of tungsten, which contains about 10% of porosity. The effect of tungsten content on the density of final hot rolled strips is shown in Figure 4.21. It has been already explained that how the presence of tungsten particles obstruct the removal of pores. These effects would increase with increasing tungsten content. The various mechanical properties determined from the tension test are compared for copper-tungsten strips containing 5%, 10%, and 20% tungsten, which were subjected to 82% thickness reduction by hot rolling. Ultimate tensile strength, percentage

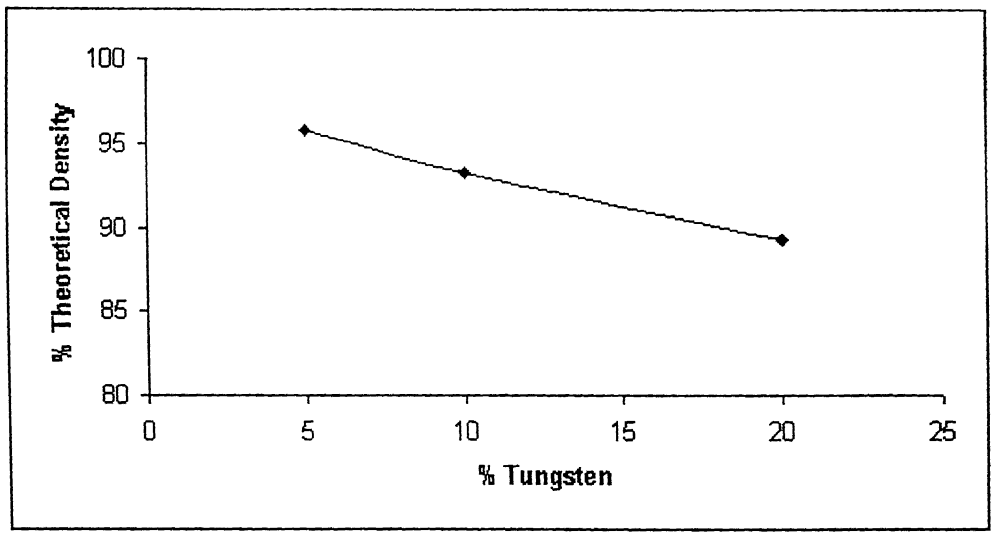

Figure 4.21: Variation of density with tungsten content of Cu-W composite strips hot rolled to 82% of thickness reduction

elongation and 0.2% proof strength of these copper-tungsten strips are shown in Table 4.9.

Table 4.9 Mechanical properties of Cu-W composite strips hot rolled to 82% thickness reduction

Composition	% Elongation	UTS, MPa	0.2% proof strength M Pa
95Cu-5W	28	216	89
90Cu-10W	23	224	92
80Cu-20W	21	281	104

Ultimate tensile strength increases with increasing tungsten content as shown in Figure 4.22. This is because tungsten is the hard phase so increasing the amount of hard second phase particles will increase tensile strength.

Figure 4.23 shows the variation of percentage elongation with tungsten content. Increasing tungsten content decreases the percentage elongation. Copper is much ductile while tungsten has very little ductility. So copper-tungsten strip with higher tungsten content or lower copper content will have lower percentage elongation. Also it is known that percentage elongation is much more dependent on the presence of porosity which tends to be greater for the copper-tungsten composite strip containing higher percentage of tungsten as illustrated earlier.

Microhardness values of copper-tungsten composites with varying compositions are shown in Table 4.10. It is nearly same for all the copper-tungsten composites. The hardness was measured by making the indent at the Cu/W interface, such that part of the

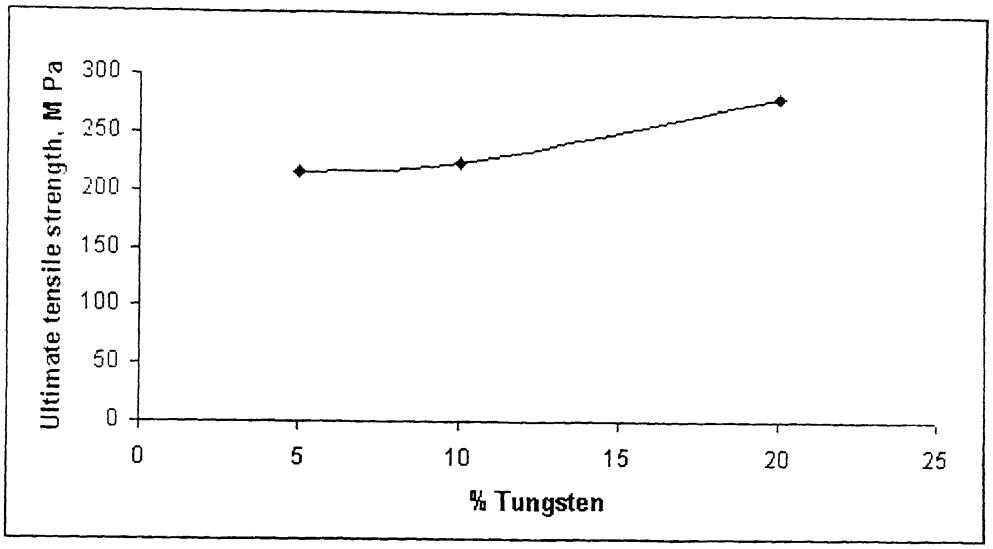

Figure 4.22: Variation of ultimate tensile strength with tungsten content of Cu-W composite strips hot rolled to 82% of thickness reduction

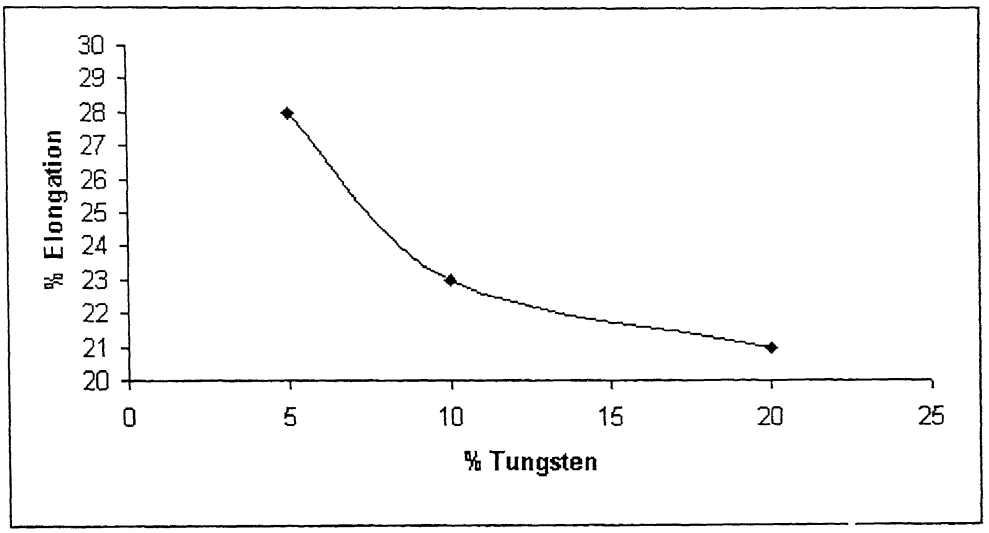

Figure 4.23: Variation % elongation with tungsten content of Cu-W composite strips hot rolled to 82% of thickness reduction

indent was in copper matrix and the remaining part in the tungsten particle. Since all the strips were hot rolled to the same thickness deformation the tungsten particles have been subjected to similar amounts of cold rolling in all the three cases. Thus similar hardness values in all the three cases are expected.

Table 4.10 Microhardness of Cu-W composite strip hot rolled to 82% thickness reduction

Composition	Microhardness, kg/mm^2
95Cu-5W	126.6
90Cu-10W	126.6
80Cu-20W	126.8

4.7 Effect of Tungsten Content on the Electrical Conductivity of Cu-W Composite Strips

The values of electrical conductivity of copper-tungsten composite strips containing 5, 10 and 20wt% of tungsten are shown in Table 4.11.

Table 4.11 Electrical conductivity of Cu-W composite strip hot rolled to 82% thickness reduction

Composition	Electrical conductivity, %IACS	Electrical conductivity calculated from mixture rule, %IACS
95Cu-5W	77	96.5
90Cu-10W	74	93.1
80Cu-20W	65	86.2

Figure 4.24 shows the variation of electrical conductivity with tungsten content. Electrical conductivity decreases almost linearly with increasing tungsten content. Tungsten is bad conductor of electricity while copper has high electrical conductivity thus with increasing tungsten content overall electrical conductivity decreases because main contribution of electrical conductivity comes from copper, which is lower in content. Porosity also affects the electrical conductivity as it reduces the area available for the flow of the current. From the percentage theoretical density it is found that copper-tungsten composite with 5 wt% of tungsten contains only ~4% porosity as compared to composite containing 20 wt% of tungsten content, which has ~10% of porosity as given in Table 4.12. The table also gives the value of percentage deterioration of electrical conductivity vis-à-vis electrical conductivity calculated from the mixture rule. It is apparent that the percentage deterioration in electrical conductivity increases as the weight percentage tungsten increase, which in turn increases the percentage porosity in the strip.

Table 4.12 Deterioration of electrical conductivity

Composition	% Porosity	% Deterioration of electrical conductivity
95Cu-5W	4.3	20.2
90Cu-10W	6.7	20.5
80Cu-20W	10.7	24.6

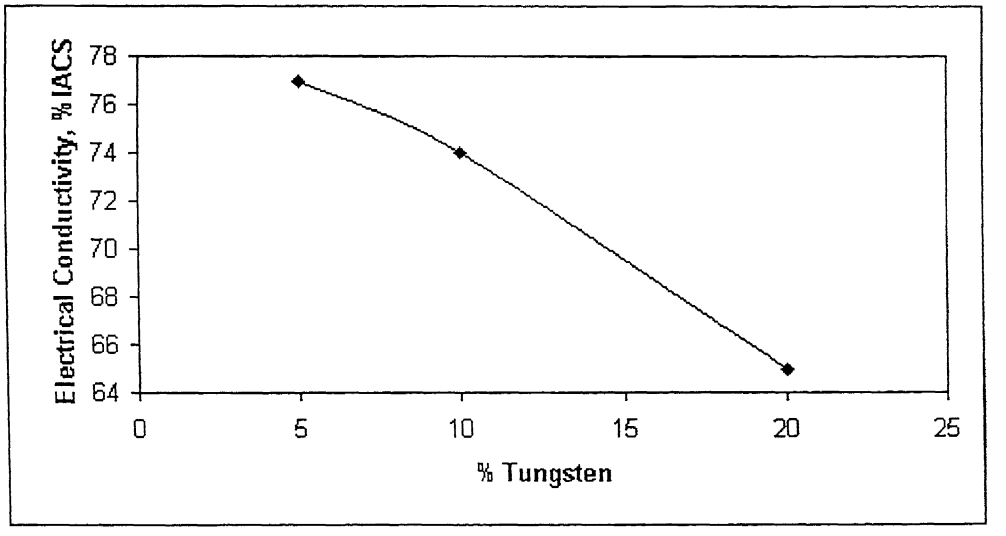

Figure 4.24: Variation electrical conductivity with tungsten content of Cu-W composite strips hot rolled to 82% of thickness reduction

CHAPTER 5

CONCLUSIONS

The following conclusions are made for the present study.

(1) It is possible to produce copper-tungsten composite strips having tungsten up to 20 wt% from high energy milled powder by the proposed Powder Metallurgy route, i.e.

Slurry making from composite powder & a binder → strip casting → sintering → hot rolling → annealing

(2) In the case of 80 wt% Cu-20 wt% W system, it is possible to produce hot rolled and annealed strip having an ultimate tensile strength of 281 MPa, 0.2% proof strength of 104 MPa and elongation of 21%, by optimizing the percent thickness reduction by hot rolling. The electrical conductivity of the strip produced is ~76% IACS. It appears to be a useful material for electrical contact applications.

(3) The densification and deformation occurring during hot rolling of porous 80 wt% Cu-20 wt% W strip could be broadly divided into three stages.

In stage I, the overall effect of hot rolling is the rearrangement and restacking of the particles. The interparticle contact area increases, but the overall contact area is not large. As a result, there is some increase in the ultimate tensile strength and practically no change in the percentage elongation of the strip. The completion of this stage occurs when the apparent density of the strip has attained a value of ~ 65% of the theoretical.

In stage II, the plastic deformation of copper particles in the composite strip becomes the predominant densification mechanism. The interparticle contact

area increases rapidly. As a result, the mechanical properties of the strip also increase rapidly. At the end of this stage, optimum mechanical properties in the strip are obtained. The apparent density of the strip is ~ 90% of the theoretical density.

During hot rolling of the 80Cu-20W strip in stage III, de-cohesion of tungsten particles from the copper matrix together with the fracturing of tungsten particles takes place. This leads to the deterioration of mechanical properties.

(4) As the tungsten content decreases in the strip, the porosity in the final hot rolled strip subjected to the same amount of thickness reduction decreases. Decrease in tungsten content also increases the percentage elongation and electrical conductivity values, while it decreases the ultimate tensile strength and 0.2% proof strength of the strip. Depending on the requirements, one may select a proper composition of the copper-tungsten strip.

CHAPTER 6

SUGGESTIONS FOR THE FUTURE WORK

(1) The mechanism of densification and deformation of copper-tungsten strip having tungsten content less than 20 wt% should be studied, and a comparision of the behaviour with that of 80Cu-20W strip should be made.

(2) The process of extrusion for the densification of porous copper-tungsten strip should be carried out, in order to investigate whether any increase in the final density of the product is possible than that obtained by hot rolling process.

(3) The wear and erosion characteristics of the copper-tungsten strip should be studied.

(4) The milling time during high-energy milling should be increased in such a way that metastable phase is formed after milling. Its effect on the final properties should be studied.

REFERENCES

[1] H. Schreiner, Powder Met. Int., 1980, 12, (1), 16-20.

[2] Y. Z. Wan, Y. L. Wang, G. X. Cheng, H. M. Tao, & Y. Cao, Powder Metall., 1998, 41, (1), 59-63.

[3] Z. Aslanoglu, Y. Karakas, & M. L. Ovecoglu, Int. J. Powder Metall., 2000, 36, (8), 35-42.

[4] ASM Metals Handbook, Vol. 7, Powder Metal Technologies & Applications, 1998, ASM International, Materials Park, OH, 1021-1030.

[5] Y. S. Shen, ASM metals Handbook, Vol. 2, Properties & selection: Non Ferrous Alloys & Special Purpose Materials, 1990, ASM International, Materials Park, OH, 1021-1030.

[6] G. Otto, ASM metals Handbook, Vol. 7, Powder Metallurgy, 1984, ASM International, Materials Park, OH, 634.

[7] P. R. Subramanian & D. E. Laughlin, Phase Diagrams of Binary Tungsten Alloys, 1991, Indian Institute of Metals, 76.

[8] K. Tousimi, A. R. Yavari, J. –H. Ahn & A. Sulpice, Mater. Sci. Forum, 1999, 307, 223-229.

[9] K. Tousimi, A. R. Yavari, J. –H. Ahn & A. Sulpice, Mater. Sci. Forum, 1999, 307, 224.

[10] K. Tousimi, A. R. Yavari, J. –H. Ahn & A. Sulpice, Mater. Sci. Forum, 1999, 307, 225.

[11] R. M. German, Powder Metallurgy Science, 1994, MPIF, Princeton, New Jersey, 274-281.

[12] R. M. German, Sintering Theory & Practice, 1996, John Wiley & Sons, Inc., 225-307.

[13] T. –H. Ihn, S. –w. Lee, & S. –K. Joo, Powder Metall., 1994, 37, (4), 283-288.

[14] J. M. Campus, & R. M. German, Advances in Powder Metallurgy and Particulate Materials, 1992, vol.3, (Proc. of 1992 PM World Congress), MPIF, 35-46.

[15] J. L. Sepuleveda & L. A. Valenzuela, Met. Powder Rep., June 1998, 24-27.

[16] K. Tousimi, A. R. Yavari, J. –H. Ahn & A. Sulpice, Mater. Sci. Forum, 1999, 307. 226.

[17] K. V. Sebastian & G. S. Tendolkar, Int. J. Powder Metall., 1979, 15, (1), 45-52.

[18] J. L. Sepuleveda & L. A. Valenzuela, Met. Powder Rep., June 1998, 25.

[19] J. L. Sepuleveda & L. A. Valenzuela, Met. Powder Rep., June 1998, 26.

[20] K. V. Sebastian, Int. J. Powder Metall. & Powder tech., 1981, 17, (4), 297-302.

[21] K. V. Sebastian & G. S. Tendolkar, Int. J. Powder Metall., 1979, 15, (1), 48.

[22] K. V. Sebastian, Int. J. Powder Metall. & Powder tech., 1981, 17, (4), 298.

[23] I. H. Moon & J. S. Lee, Powder Metall. Int., 1977, 9, (1), 23-24.

[24] I. H. Moon & J. S Lee, Powder Metall., 1979, 22, (1), 5-7.

[25] I. H. Moon & J. S Lee, Powder Metall., 1979, 22, (1), 6.

[26] W. D. Kingery, J. Appl. Phys., 1959, 30, 301.

[27] V. N. Eremenko, Yu. V. Naidich & I. A. Labrinenko, Sov. Powder Metall. Met. Ceram., 1962, 1, (4), 282.

[28] J. S. Hirschhorn, Introduction to Powder Metallurgy, 1969, APMI, Princeton, New Jersey, 116.

[29] J. A. Belk, M. R. Edwards, W. J. Farrel, & B. K. Mullah, Powder Metall., 1993, 36, (4), 293-296.

[30] J. A. Belk, M. R. Edwards, W. J. Farrel, & B. K. Mullah, Powder Metall., 1993, 36, (4), 294.

[31] J. A. Belk, M. R. Edwards, W. J. Farrel, & B. K. Mullah, Powder Metall., 1993, 36, (4), 295.

[32] A. Mishima, K. Tokumoto & S. Sakaguchi, Nippon Tungsten review, 1998, 30, 7-12.

[33] A. Mishima, K. Tokumoto & S. Sakaguchi, Nippon Tungsten review, 1998, 30, 9.

[34] I. H. Moon, E. P. Kim, & G. Petzow, Powder Metal., 1998, 41, 910, 51-57.

[35] A. Mishima, K. Tokumoto & S. Sakaguchi, Nippon Tungsten review, 1998, 30, 11

[36] C. Suryanarayana, Non-Equilibrium Processing of Materials, 1999, Pergamon Press, New York, 49-81.

[37] M. S. EI-Eskandarny, Mechanical Alloying for fabrication of Advanced Engineering Materials, 2001, Noyes Publications, New York, 1-21.

[38] I. H. Moon, E. P. Kim, & G. Petzow, Powder Metal., 1998, 41, 910, 52.

[39] J. S. Benjamin & J. E. Volin, Metall. Trans., 1974, 5, 1929.

[40] I. H. Moon, E. P. Kim, & G. Petzow, Powder Metal., 1998, 41, 910, 53.

[41] I. S. Ahn, B. S. Kim & I. H. Moon, Advances in Powder Metallurgy & Particulate Materials, 1, (4), 1995, 209-217.

[42] K. V. Sebastian & G. S. Tendolkar, Powder Metall. Int., 1979, 11, 62.

[43] E. N. Aqua & C. I. Whitman, Modern Developments in Powder Metallurgy, 15, 1985, MPIF, New Jersey, 489-506.

[44] F. V. Lenel, Powder Metall., Principles & Applications, 1980, MPIF, New Jersey.

[45] B. L. Mordike, J. Kaczmar, M. Kielbinski & K. U. Kainer, Powder Metall. Int., 1991, 23, (2), 91-95.

[46] B. I. Edelson, W. M. Baldwin, transactions of the ASM, 1962, 55, 230-250.

[47] B. L. Mordike, J. Kaczmar, M. Kielbinski & K. U. Kainer, Powder Metall. Int., 1991, 23, (2), 92.

[48] B. L. Mordike, J. Kaczmar, M. Kielbinski & K. U. Kainer, Powder Metall. Int., 1991, 23, (2), 93.

[49] B. L. Mordike, J. Kaczmar, M. Kielbinski & K. U. Kainer, Powder Metall. Int., 1991, 23, (2), 94.

[50] T. W. Clyne & P. J. Withers, An Introduction to Metal Matrix Composites, 1993, Cambridge university Press, 336.

[51] J. S. Hirschhorn, Introduction to Powder Metallurgy, 1969, APMI, Princeton, New Jersey, 244-245.

[52] Tension Testing of Metallic Materials, E8-61T ASTM Standards, Part-3, 165, 1961, Philadelphia, American Society of Testing & Materials.

[53] Howard E. Boyer, & Timothy L. Gall, Metals Handbook, Desk Edition, 1984, ASM, Metals Park, Ohio, 20.20.

[54] J. Kaczmar, Powder Metal., 1989, 32, 3, 175.

[55] S. Bhargava and R. K. Dube, Metall. Trans. A, 1988, Vol. 19A, 1205-1211.

[56] John A. Schey, Introduction to Manufacturing Processes, 1977, McGraw Hills, 95.

[57] F. B. Pickering and S. W. Robinson, in "Inclusions', F. B. Pickering, 1979, The Institution of Metallurgists, London, 127.

[58] J. A. Belk, M. R. Edwards, W. J. Farrel, & B. K. Mullah, Powder Metal., 1993, 36, (4), 293.

[59] I. H. Moon, E. P. Kim, & G. Petzow, Powder Metal., 1998, 41, 910, 51.